TARTU OBSERVATORY
space research centre

The Effelsberg–Bonn HI Survey

Urmas Haud

The Effelsberg–Bonn HI Survey

In Germany

- Aims
- Technical setup
- Data reduction stages

In Estonia

- Weights
- Baseline
- Noise

Aims of the survey (AN **332**, 6, 637, 2011)

Milky Way survey

- Complete census of all HVCs
  - Ultra-compact HVCs
  - HVC head-tail structures
- Multiphase structure of the extra-planar gas
  - Interaction of HVCs with IVCs and the Milky Way gas
- HI mass and size spectrum of clouds
  - cold and dense clumps in a low density environment
- HI shells
  - Feedback processes between the stars and the ISM
- Soft X-ray absorption
  - Foreground for extragalactic observations

Extragalactic survey

- The low-mass part of the HI mass function
  - In SDSS area the HI mass sensitivity of $M(\text{HI}) = 3 \cdot 10^7\ M_\odot$ at the distance of the Virgo cluster
- The local baryon budget
  - Statistical census of HI in the local universe
- High quality HI data of bright galaxies
- Isolated HI clouds in the intergalactic medium
- Search for galaxies close to low red–shift Lyα absorbers
- The imprint of environmental conditions on galaxies

Technical setup (ApJS 188, 488, 2010)

- Effelsberg 100 m telescope
- Seven-feed-array receiver with 14 receiving channels
  - 2 polarizations for each feed
- Digital FFT-type spectrometers
  - Bandwidth of 100 MHz
  - 16384 spectral channels
  - In-band frequency switching
    - Frequency shift of 4(3) MHz
- 5 × 5 degree fields are measured with on-the-fly R.A.–Dec. scanning (scan, sub-scan, dump)
  - Scan speed is 4´ per second
  - Full spectra are stored every 0.5 s
- Three observing periods
  - R.A. scans (completed)
  - Dec. scans (in progress for Dec > 30°)
  - Additional scans in SDSS area (no money)
- Do not read papers, published before 2010!

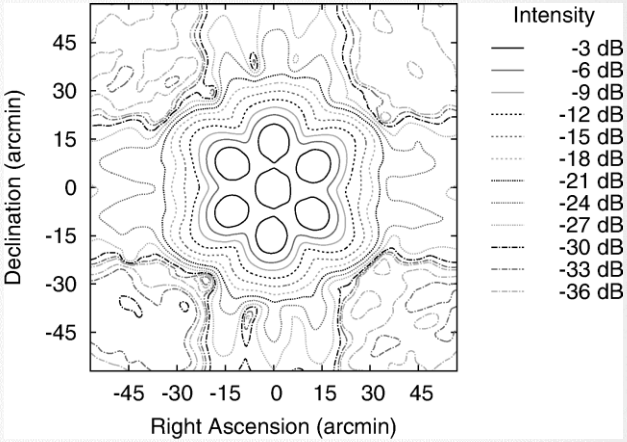

Galactic HI surveys (A&A 585, A41, 2016)

	LAB	GASS	GALFA	EBHIS	
Decl.	Full	≤ 1	-1 … 38	≥ -5	deg
ϑ_{FWHM}	36	16.1	4.0	10.8	arcmin
$\lvert v_{lsr} \rvert$	≤ 460	≤ 470	≤ 750	≤ 600	km s^{-1}
Δv	1.03	0.82	0.18	1.29	km s^{-1}
δv	1.25	1.00	0.18	1.44	km s^{-1}
T_{rms}	80	57	325	<90	mK
T_{rms}^{norm}	89	57	140 60 (ALFALFA 7 074 deg^2) 33 (AGES, 200 deg^2)	<108	mK

ϑ_{FWHM} - angular resolution, v_{lsr} - velocity interval, Δv - channel separation,
δv - spectral resolution, T_{rms} - brightness temperature noise level,
T_{rms}^{norm} - normalized noise level at a common spectral resolution of 1 km s^{-1}

Extragalactic surveys (A&A 569, A101, 2014)

	HIPASS	ALFALFA	EBHIS	
Decl.	≤ 25	-0 … 36 7.5^h ≤ R.A. ≤ 16.5^h 22.0^h ≤ R.A. ≤ 3.0^h	≥ -5	deg
Area	29 343	7 074	22 424	deg^2
ϑ_{FWHM}	15.5	3.5	10.8	arcmin
δv	26.4	5.4	10.24	km s^{-1}
v_{lsr}	-1 280 … 12 700	-1 600 … 18 000	-2 000 … 18 000	km s^{-1}
Source density	0.2	5.8 (2 800 deg^2)	~0.2	deg^{-2}

Fundamentals – 1

- For a black body in thermal equilibrium with its surroundings, the specific intensity of the thermal radiation is $I_\nu = B_\nu(T)$ (Planck function)
  - At radio frequencies $h\nu/kT \ll 1$ ➔
  - Raleigh-Jeans law $B_\nu(T) = 2kT\nu^2/c^2$ ➔
  - **Brightness temperature** $T_b = I_\nu \lambda^2/2k$
- **Antenna temperature** $T_A = \frac{1}{\Omega_A} \oiint_{4\pi} F(\theta,\varphi) \cdot T_b(\theta,\varphi) d\Omega$
  - Ω_A - the antenna solid angle
  - $F(\theta,\varphi)$ - the power pattern of the antenna

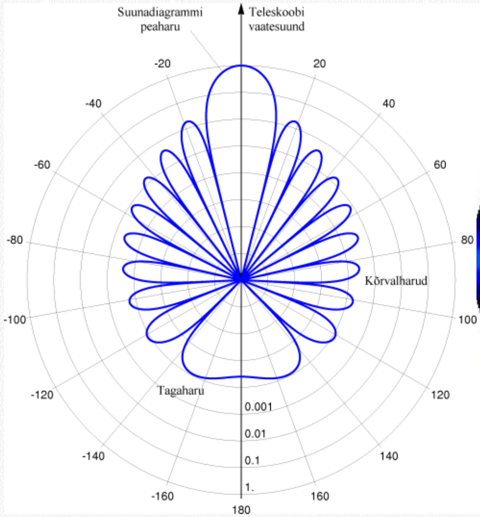

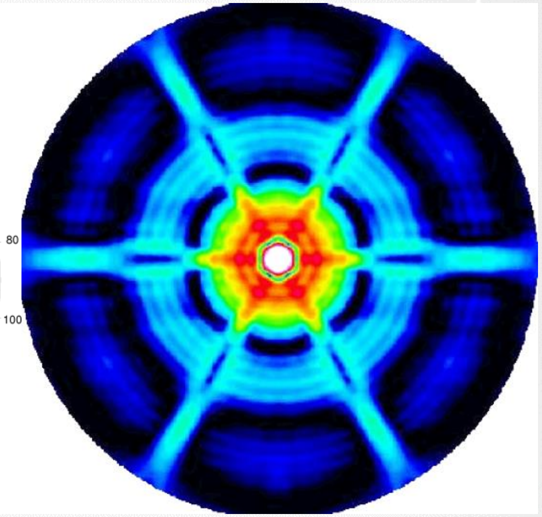

Fundamentals – 2

- The receiving system consists of an antenna, a transmission line and a receiver ➔
- **System temperature**

$$T_{sys} = (T_A + T_{AP})e_L + T_{LP}(1 - e_L) + T_r$$

  - T_{AP} - temperature due to the physical temperature of the antenna
  - T_{LP} - temperature due to the transmission line
  - T_r - noise temperature of the receiver
  - e_L - line thermal efficiency

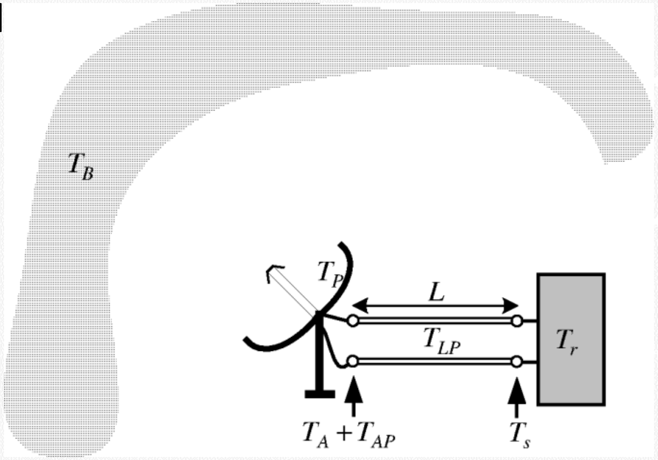

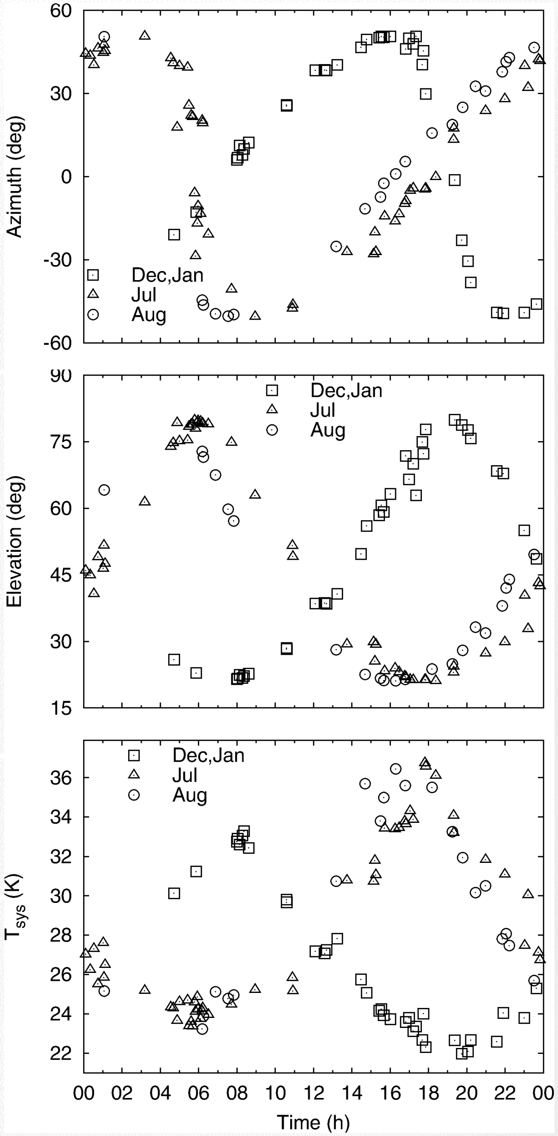

Data reduction scheme (ApJS 188, 488, 2010)

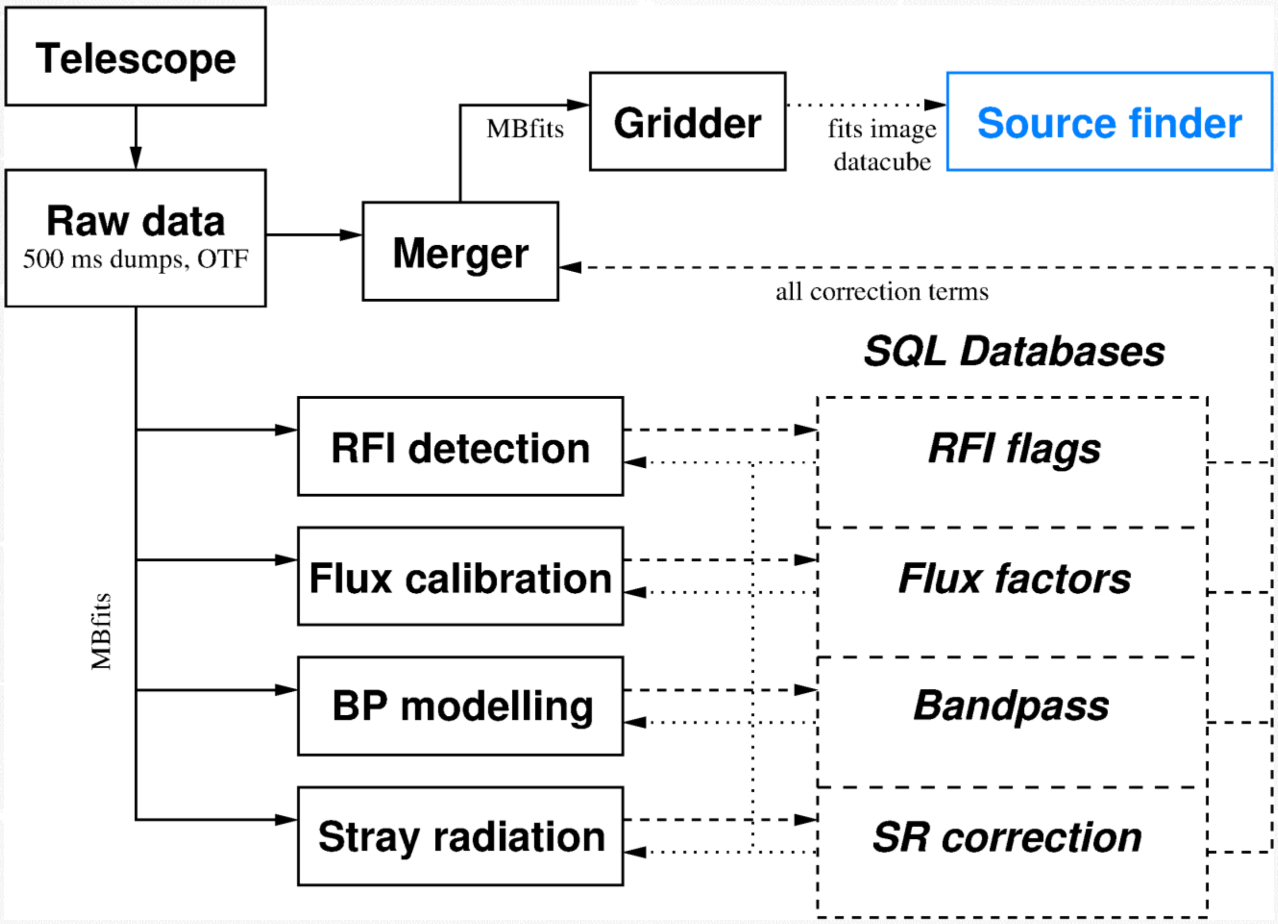

RFI (http://pos.sissa.it/cgi-bin/reader/conf.cgi?confid=107, id. 42)

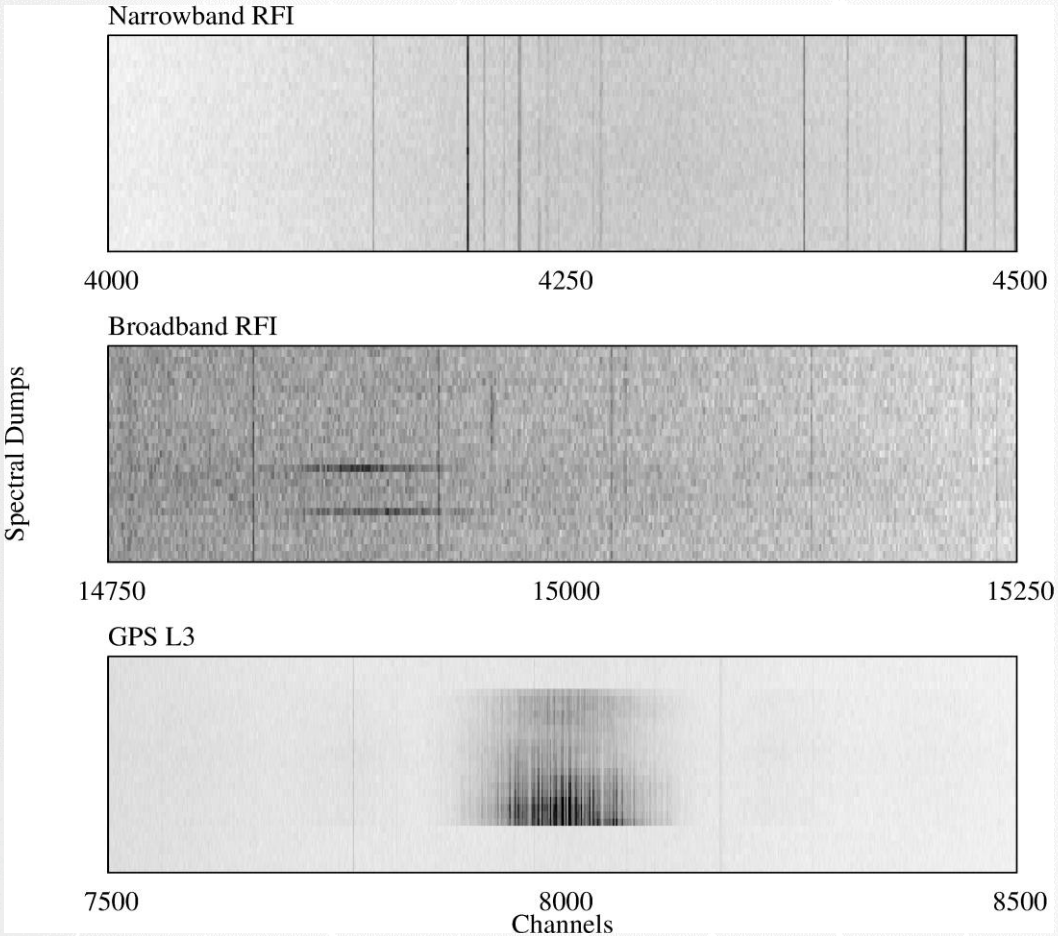

- Near-constant narrow-band spikes, typically affecting one or two spectral channels
- Intermittent broad-band events affecting a hundred up to thousands of spectral channels
- Extremely strong RFI caused by the L3 mode of the GPS satellite system

RFI flagging (A&A 585, A41, 2016)

- 14 independent measurements of the RFI environment at any time ➔ Matched filtering, adapted to the typical appearance of RFI in a time-frequency plots
  - Narrow-band RFI
    - Average 2 polarizations for each feed & each sub-scan in time ➔ 7 spectra per sub-scan
    - Remove large scale components by subtracting a median-filtered version of the spectrum
    - Require that a channel exceeds a lower threshold T_N in N feeds simultaneously
    - Subtract the RFI if the criterion is met for any $N = 4 \cdots 7$ $\left(\left[1-\Phi\left(T_N\right)\right]^N = 1-\Phi\left(T_1\right)\right)$
  - Broad-band RFI
    - Smooth the data in spectral domain with a Gaussian filter adapted to the typical RFI
    - Apply a three-point median filter in the time domain to suppress persistent signals
    - Perform combinatorial thresholding in time domain across the seven feeds & flag the RFI
  - GPS L3
    - Always at 1381.05 MHz ➔ usually does not affect the velocities $|V_{\mathrm{LSR}}| < 600\ \mathrm{km/s}$
    - Compare the RMS in a 1 MHz window around RFI to the RMS in neighboring frequencies
    - If the RMS differs by at least a factor of two, flag a 10 MHz window around RFI
- Manual inspection of each observation
  - Data 32-fold binned in frequency
  - Each spectral dump divided by the median spectrum of the current sub-scan
  - Images of the time-frequency plane & flagging by a mouse click

Line emission (A&A 540, A140, 2012)

- Measured spectral density function in arbitrary units

$$P^{[\mathrm{cal}]}(\nu) = G(\nu)\left(T_{\mathrm{A}}(\nu) + T_{\mathrm{sys}'}^{[\mathrm{cal}]}(\nu)\right)$$

  - $G(\nu)$ - frequency-dependent gain of the telescope and the receiving system
  - Antenna temperature: $T_{\mathrm{A}} = T_{\mathrm{A}}^{\mathrm{line}} + T_{\mathrm{A}}^{\mathrm{cont}}$
  - Noise contributions: $T_{\mathrm{sys}'}^{[\mathrm{cal}]} = T_{\mathrm{bg}} + T_{\mathrm{atm}} + T_{\mathrm{spill}} + T_{\mathrm{sw}} + T_{\mathrm{loss}} + T_{\mathrm{rx}}[+T_{\mathrm{cal}}]$
    - T_{bg} - microwave and galactic backgrounds
    - T_{atm} - atmospheric emission
    - T_{spill} - ground radiation (spillover and scattering)
    - T_{sw} - standing wave pattern (a semi-periodic variation in the spectral bandpass)
    - T_{loss} - losses in feed, ohmic losses
    - T_{rx} - receiver noise temperature
    - T_{cal} - injected noise using a noise diode $\left(T_{\mathrm{cal}} \approx 0.2 T_{\mathrm{sys}'}\right)$
- Must be calibrated in terms of
  - Flux density values and
  - Frequency-dependent bandpass shape $G(\nu)$

Flux calibration (ApJS 188, 488, 2010)

- Absolute flux calibration by using IAU standard calibration sources
  - Well-defined HI regions in the Milky Way
    - usually S7 (l = 132°, b = -1° – circumpolar for Effelsberg)
    - sometimes S8 (l = 207°, b = -15°)
- Slight dependence on time has been fitted with a third-order polynomial
- Gain factor $g \equiv G(v_{\mathrm{lsr}} = 0)$ is obtained with an accuracy of 2.5%

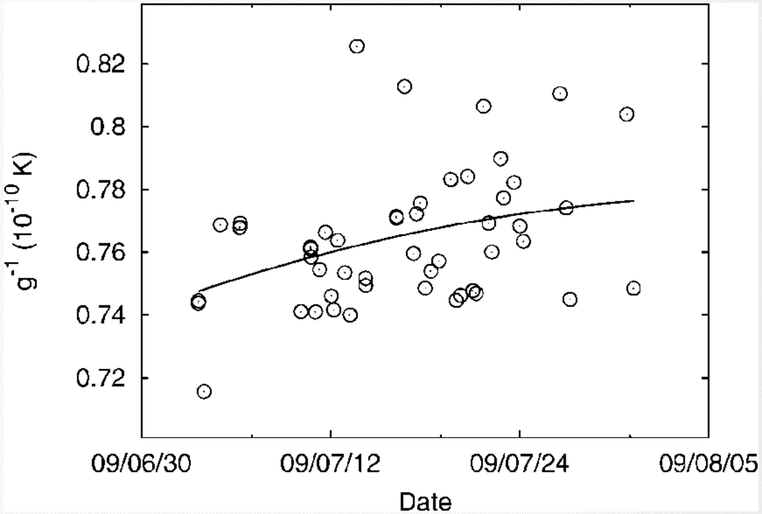

Bandpass curve (A&A 540, A140, 2012)

- Position switching – for 21-cm line no suitable OFF position
- Frequency switching – receiver has a significant bandpass ripple (SW)
- Direct determination of the bandpass curve (background and gain must not vary over the course of the observation)
  - Every second dump includes T_{cal}

$$P_i^{\mathrm{cal}} - P_i = G\left(T_{i,\mathrm{A}} + T_{i,\mathrm{sys}'}^{\mathrm{cal}} - T_{i,\mathrm{A}}^{'} - T_{i,\mathrm{sys}'}^{'}\right)$$

$$= G\left(T_{\mathrm{cal}} + \Delta T_{\mathrm{A}} + \Delta T_{\mathrm{sys}'}\right)$$

$$\Delta T_{\mathrm{A}} + \Delta T_{\mathrm{sys}'} \ll T_{\mathrm{cal}}$$

  - When averaging over ~1000 dumps

$$G = \left\langle \frac{P^{\mathrm{cal}} - P}{T_{\mathrm{cal}} + \Delta T_{\mathrm{A}} + \Delta T_{\mathrm{sys}'}} \right\rangle_t \approx \frac{\left\langle P^{\mathrm{cal}} - P \right\rangle_t}{T_{\mathrm{cal}}}$$

$$T_{\mathrm{A}} + T_{\mathrm{sys}'} = \frac{P T_{\mathrm{cal}}}{\left\langle P^{\mathrm{cal}} - P \right\rangle_t} = \frac{P^{\mathrm{cal}} T_{\mathrm{cal}}}{\left\langle P^{\mathrm{cal}} - P \right\rangle_t} - T_{\mathrm{cal}}$$

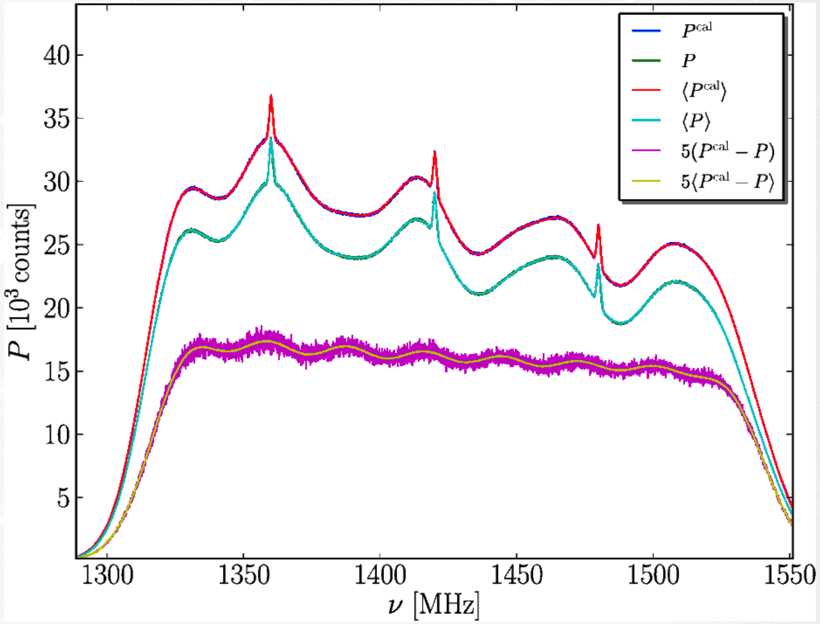

2-D baseline fitting (A&A 585, A41, 2016)

- To extract the pure spectral line contribution:
  - Source flagging:
    - LAB & later EBHIS for the Milky Way emission
    - HyperLEDA for extragalactic HI objects (http://leda.univ-lyon1.fr/)
    - NVSS for strong continuum sources (AJ 115, 1693, 1998)
    - Weaker continuum sources removed by subtracting the average T_{sys} level from each spectral dump
    - Iterative flagging of 3σ outliers
  - Polynomial baseline in time-frequency plane

$$y_{\mathrm{b}} = \sum_{i,j\geq 0} \alpha_{i,j} f^{i} t^{j}$$

    - Data fitting on tiles of 1024 spectral channels times the number of dumps per sub-scan (≈ 40)
    - Interleaved tiles (overlap 512 channels) and interpolation with sigmoid thresold
    - $i = 10, j = 2$, if $i \neq j$ only $\alpha_{1,1} \neq 0$
  - Iterations for adjusting the source flags

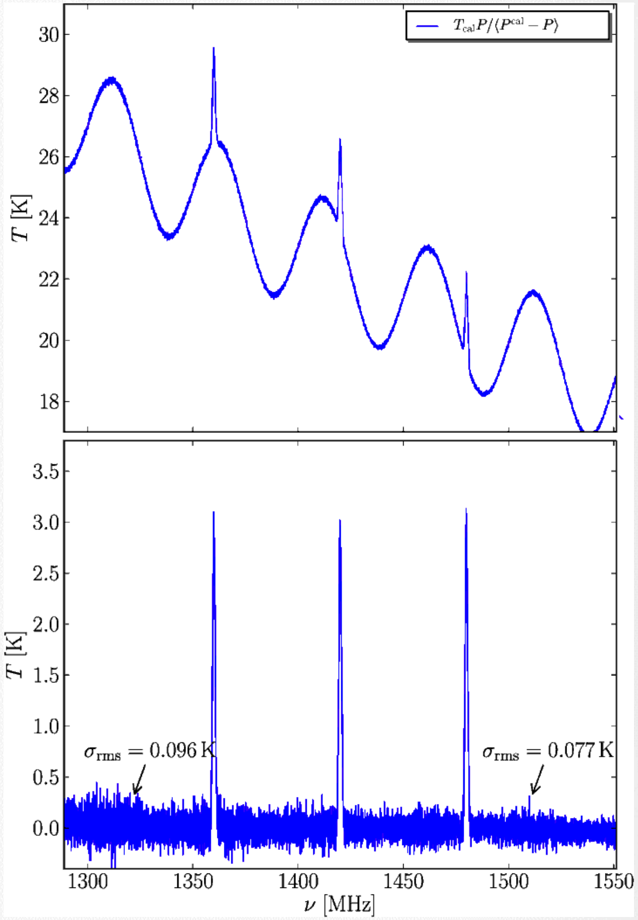

Stray-radiation (A&A 585, A41, 2016)

- $$T_A = \frac{1}{\Omega_A} \oint\!\!\oint_{4\pi} F(\theta,\varphi) \cdot T_b(\theta,\varphi)\, d\Omega$$
  - T_A is time- and frequency-dependent
  - The horizon must be taken into account
  - Ground reflectivity must be taken into account
  - Atmospheric attenuation and refraction need to be considered
- In most cases it is impossible to determine accurate absolute side-lobe levels
- The strategy is to improve the SR corrections by successive approximations, modifying antenna parameters, the correction algorithm itself and the estimate for the brightness temperature distribution

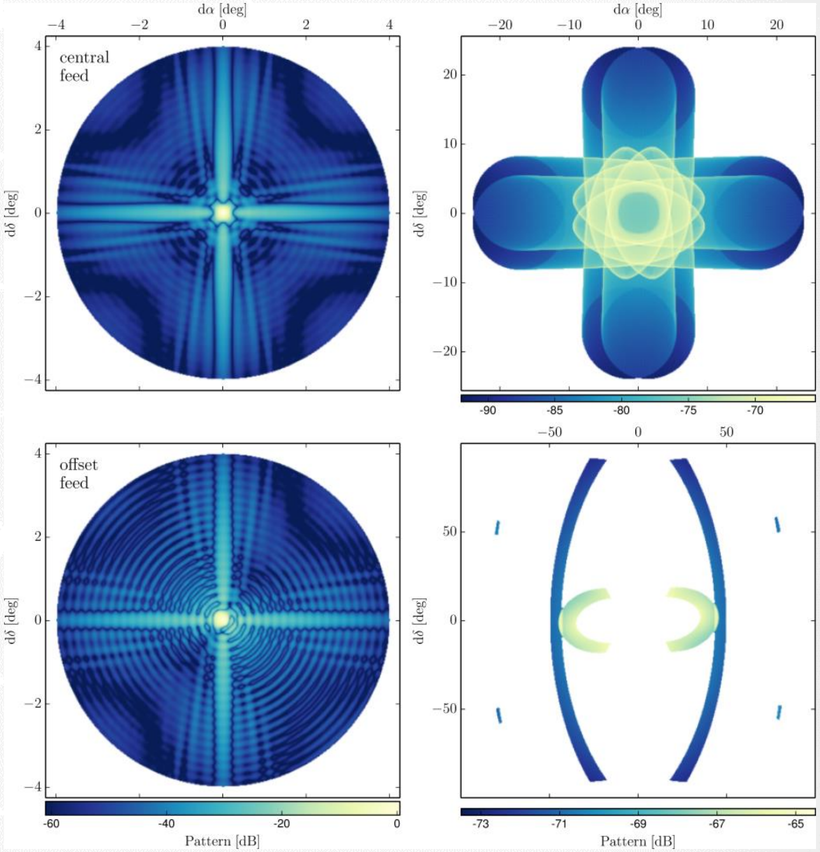

Stray-radiation correction

- The correction in several low column density regions at higher Galactic latitudes is greater than the reconstructed column densities in these fields.

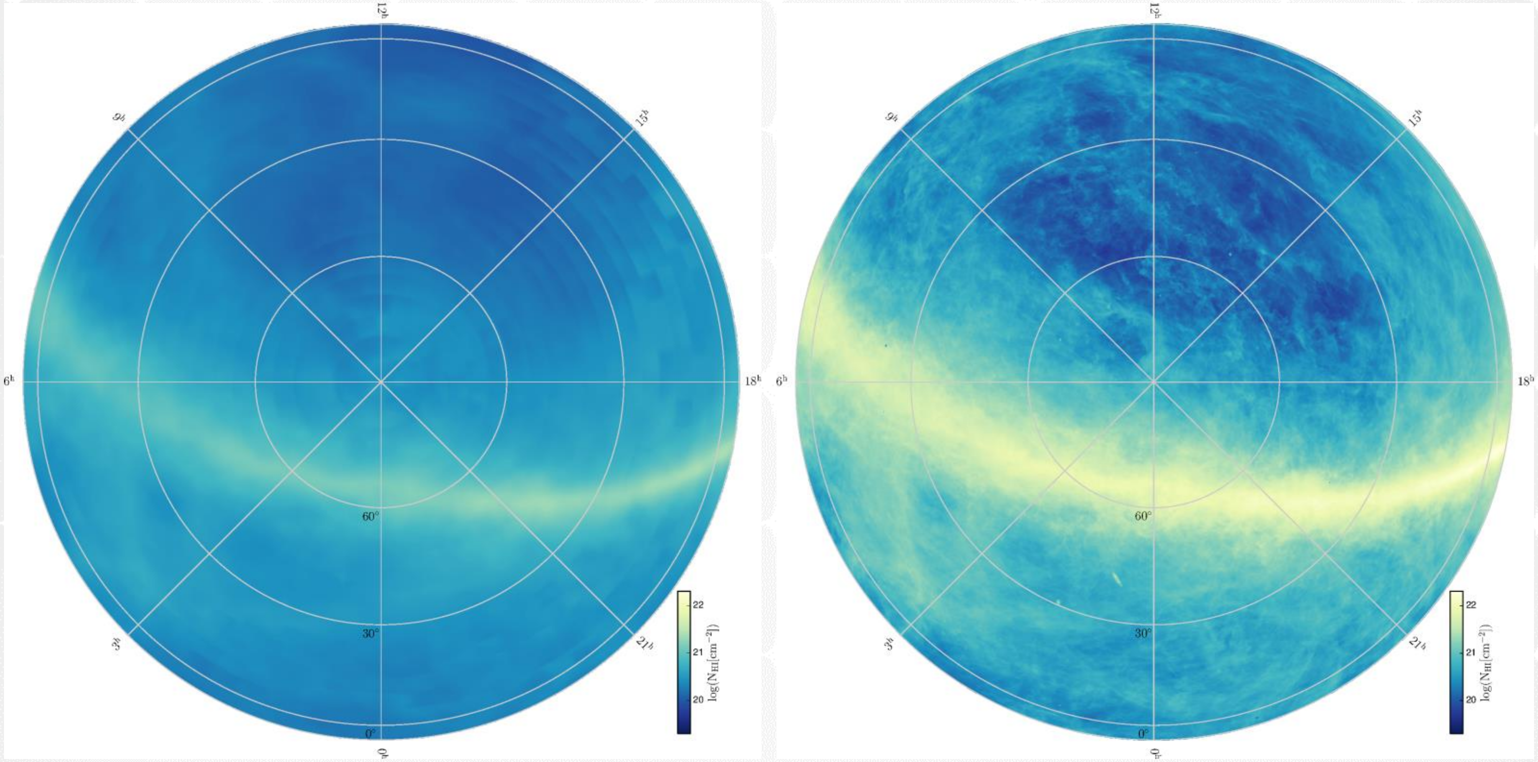

Gridding

- Weighted interpolation with a Gaussian kernel
  - The T_{sys}-based weighting scheme improves the final RMS level by about 1 to 2%.
- HEALPix – Hierarchical Equal Area and isoLatitude Pixelization (ApJ 622, 759, 2005)
  - The base resolution comprises 12 pixels in three rings around the poles and the equator
  - Rank of the pixelization $k = 10$
  - Number of divisions along the side of a base-resolution pixel $N_{\mathrm{side}} = 2^k = 1024$
  - Total number of pixels $N_{\mathrm{pix}} = 12N_{\mathrm{side}}^2 = 12\,582\,912$
  - Angular resolution $\theta_{\mathrm{pix}} = \sqrt{\frac{3}{\pi}}\frac{3600'}{N_{\mathrm{side}}} \approx 3.44'$
  - http://cdsarc.u-strasbg.fr/viz-bin/qcat?J/A+A/585/A41
- https://www.astro.uni-bonn.de/hisurvey/AllSky_profiles/

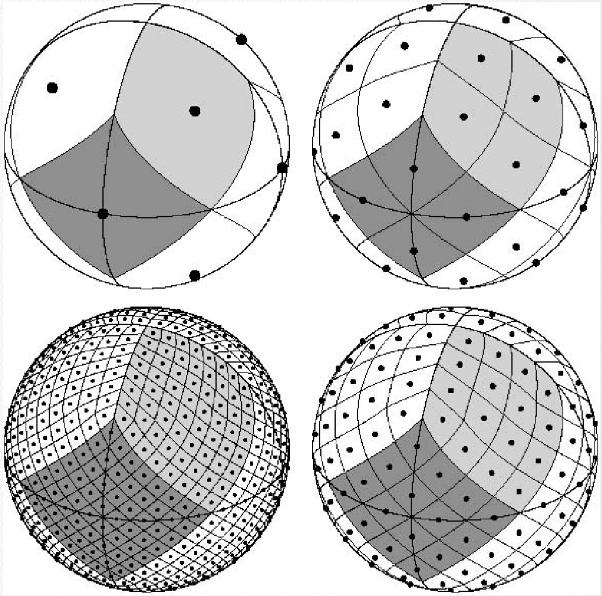

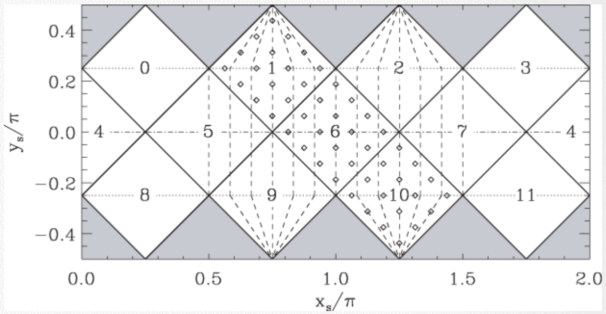

Surveys in numbers

GASS

- 6 655 155 T_b, RMS and flags profiles
  - 1 213 spectral channels in each
  - 81 192 891 000 bytes
- 60 403 345 Gaussians
  - $6^\mathrm{d}5^\mathrm{h}5^\mathrm{m}8^\mathrm{s}$ for full decomposition on 8 cores of Dell R910 server
  - 1 928 851 440 bytes

EBHIS

- 6 864 586 T_b and W profiles
  - 935 spectral channels in each
  - 52 170 853 600 bytes
- 57 500 872 Gaussians
  - $6^\mathrm{d}22^\mathrm{h}12^\mathrm{m}36^\mathrm{s}$ for full decomposition on 8 cores of Dell R910 server
  - 1 874 271 120 bytes

Weights

- Weight profiles $W_i(\nu)$
  - From radiometer equation

$$T_{\mathrm{rms},i}(\nu) = T_{\mathrm{sys},i}(\nu) \cdot \frac{K_\mathrm{s}}{\sqrt{\Delta\nu \cdot t_\mathrm{int}}} \qquad W_i = T_{\mathrm{rms},i}^{-2}$$

    - K_s – sensitivity constant
    - $\Delta\nu$ – channel frequency-spacing
    - t_int – integration time
  - RFI flags
  - Subtraction of different non-HI contributions
  - A number of dumps contribute to each pixel
- $\mathrm{RMS} = 1/\sqrt{W}$, scaled to T_b amplitude

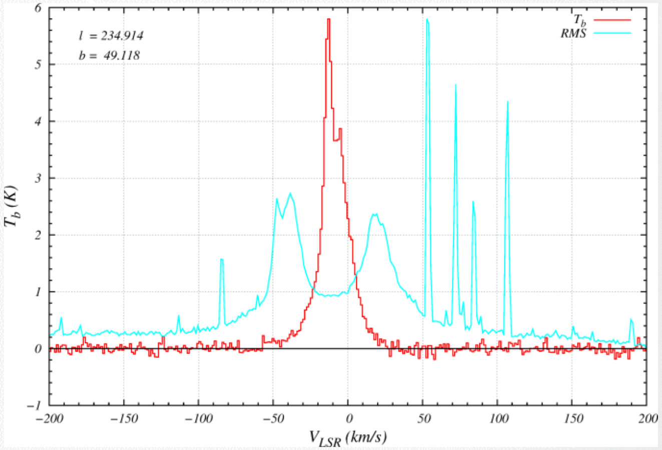

Weights

- Weight profiles $W_i(\nu)$
  - From radiometer equation

$$T_{\mathrm{rms},i}(\nu) = T_{\mathrm{sys},i}(\nu) \cdot \frac{K_\mathrm{s}}{\sqrt{\Delta\nu \cdot t_\mathrm{int}}} \qquad W_i = T_{\mathrm{rms},i}^{-2}$$

    - K_s – sensitivity constant
    - $\Delta\nu$ – channel frequency-spacing
    - t_int – integration time
  - RFI flags
  - Subtraction of different non-HI contributions
  - A number of dumps contribute to each pixel
- $\mathrm{RMS} = 1/\sqrt{W}$, scaled to T_b amplitude

"I messed up. I not only forgot to apply the LSR correction (to $T_{rms,i}$), I even forgot to apply the 4-MHz shift for half the spectra"

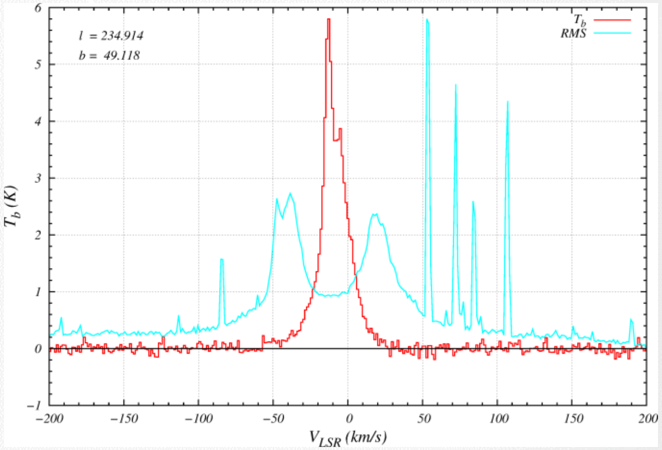

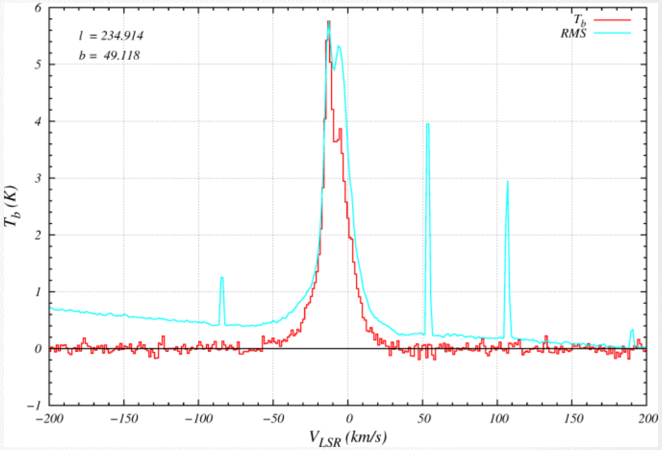

Baselines – 1

- In the first decomposition the number of negative Gaussians was 5.4 times higher than expected

Baselines – 1

- In the first decomposition the number of negative Gaussians was 5.4 times higher than expected
- On average all profiles were 10 mK below the $T_{\mathrm{b}} = 0$ level

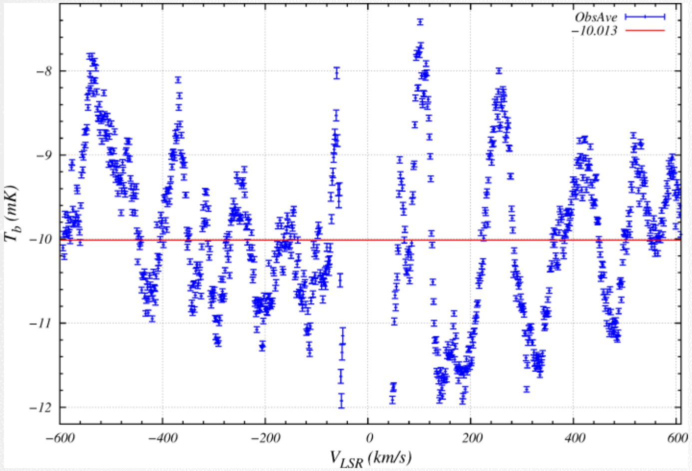

Baselines – 1

- In the first decomposition the number of negative Gaussians was 5.4 times higher than expected
- On average all profiles were 10 mK below the $T_{\mathrm{b}} = 0$ level
- The size of each Gaussian has been defined as the area under it in the range of the velocities of the profile.

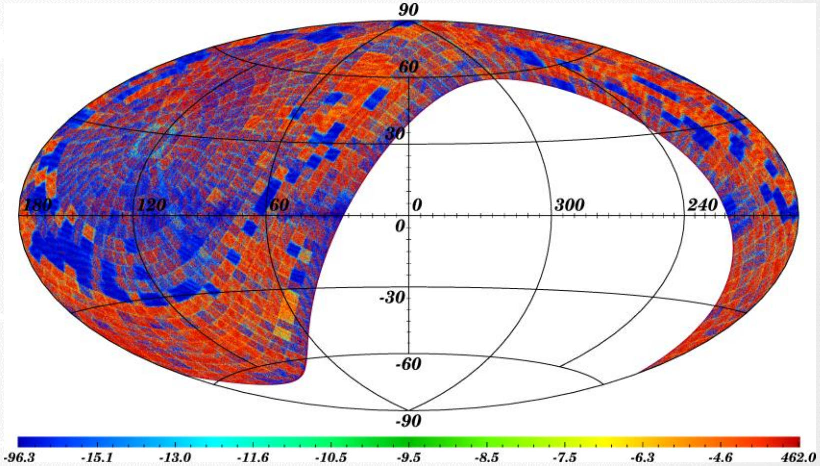

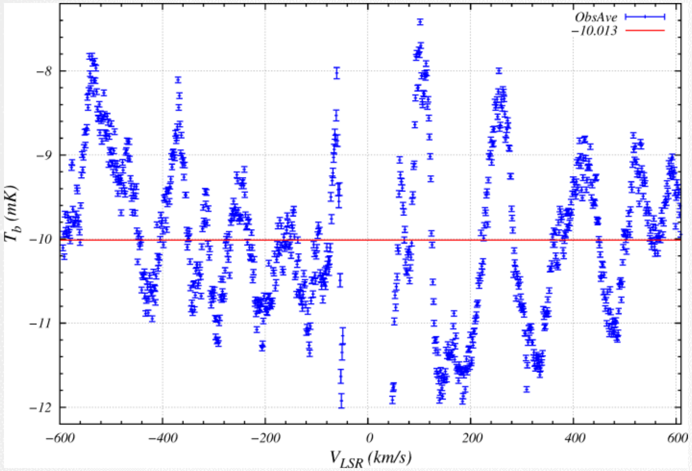

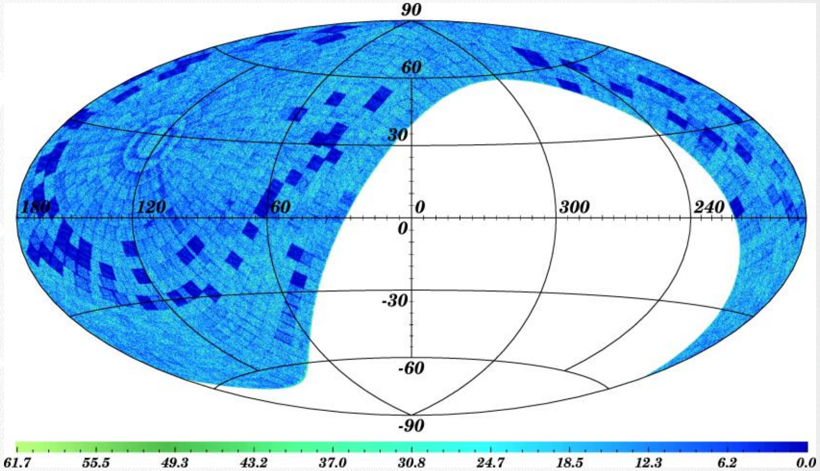

Baselines – 2

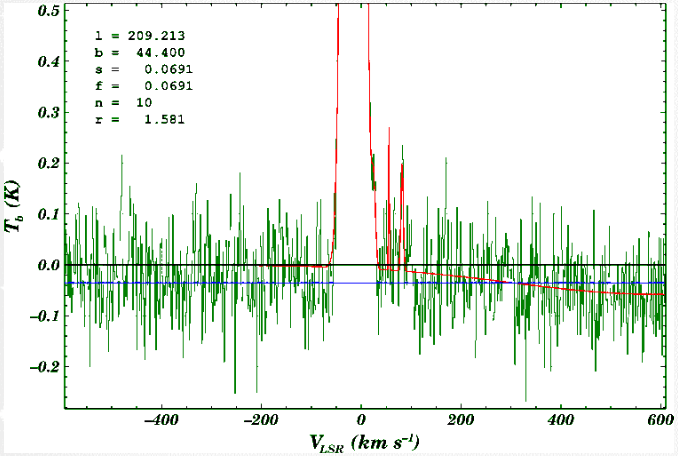

l = 209.213
b = 44.400
s = 0.0691
f = 0.0691
n = 10
r = 1.581
T_b (K)
V_{LSR} (km s^{-1})

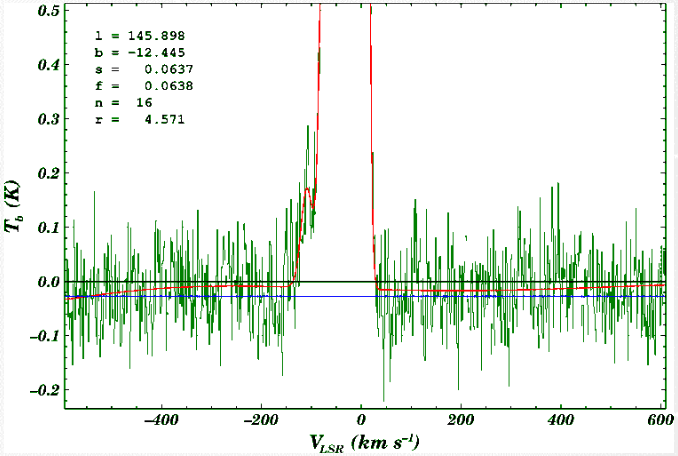

l = 145.898
b = -12.445
s = 0.0637
f = 0.0638
n = 16
r = 4.571
T_b (K)
V_{LSR} (km s^{-1})

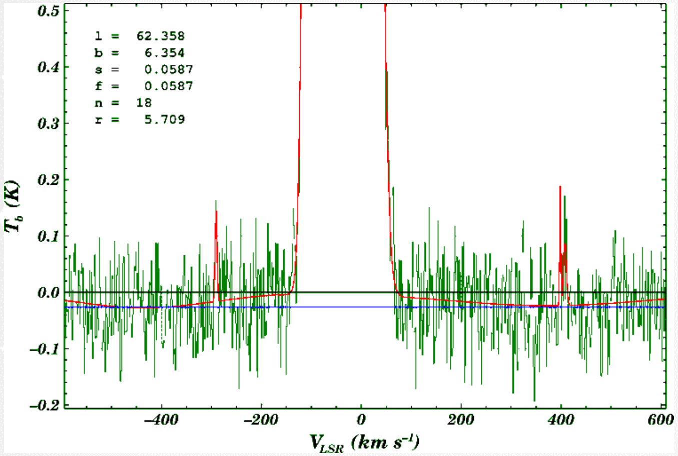

l = 62.358
b = 6.354
s = 0.0587
f = 0.0587
n = 18
r = 5.709
T_b (K)
V_{LSR} (km s^{-1})

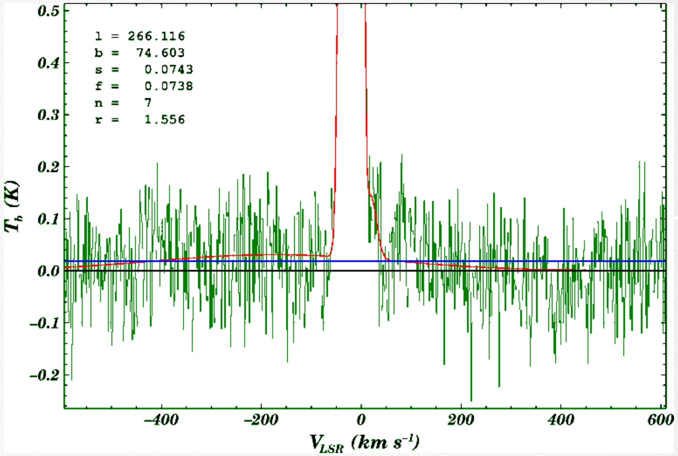

l = 266.116
b = 74.603
s = 0.0743
f = 0.0738
n = 7
r = 1.556
T_b (K)
V_{LSR} (km s^{-1})

Baselines – 3

- "If one uses noisy weight spectra to compute a linear weighted average, a bias is introduced.
- The solution is first to denoise the weight spectra.
  - I used subscan-averaged T_{sys} spectra for weighting.
  - I could try to use spectral smoothing instead (e.g., 4 channels wide Gaussian filter)."

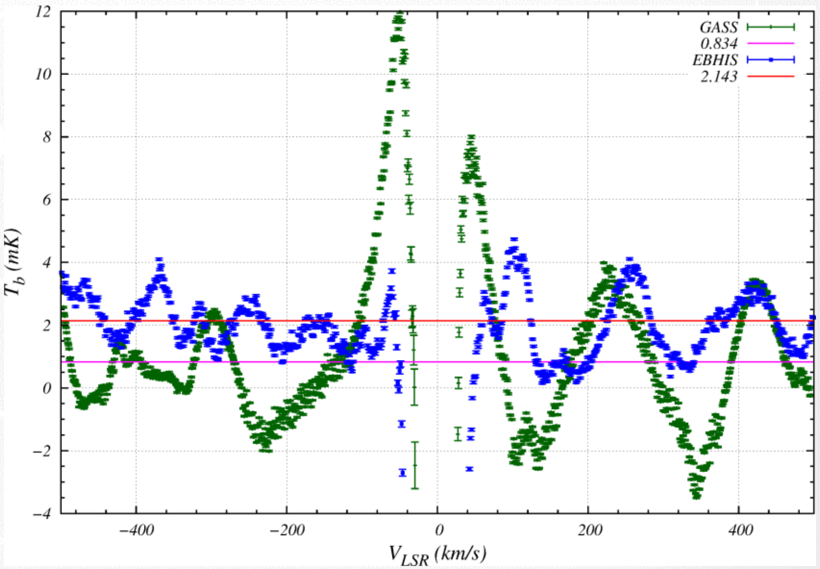

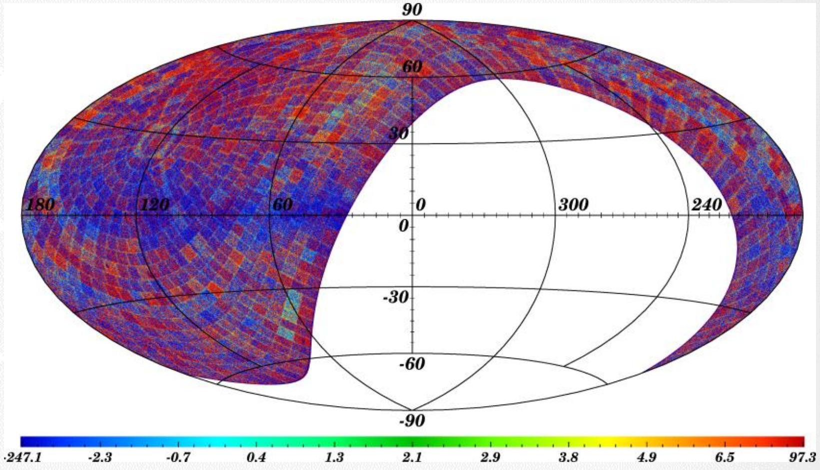

Noise – 1

- Some noise peaks are intentionally fitted with Gaussians. In EBHIS:
  - most noise components are unexpectedly wide (WNG – red boxes),
  - extremely narrow components have also appeared (NNG – blue boxes).
- Vertical enhancements correspond to the baseline oscillations

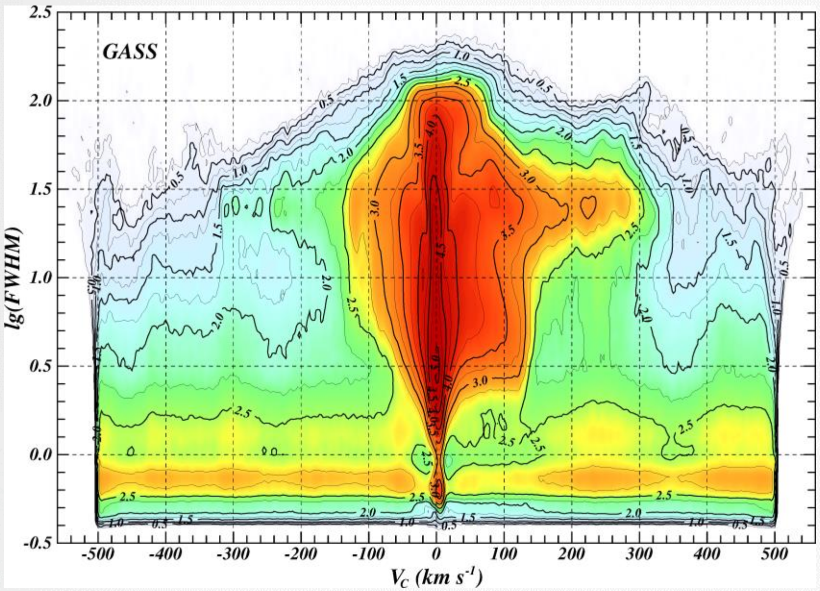

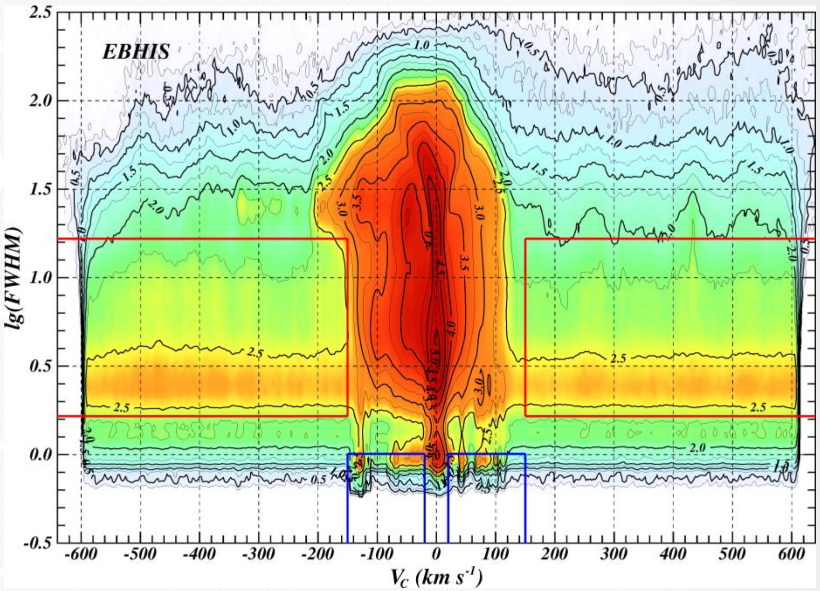

Noise – 1

- Some noise peaks are intentionally fitted with Gaussians. In EBHIS:
  - most noise components are unexpectedly wide (WNG – red boxes),
  - extremely narrow components have also appeared (NNG – blue boxes).
- Vertical enhancements correspond to the baseline oscillations

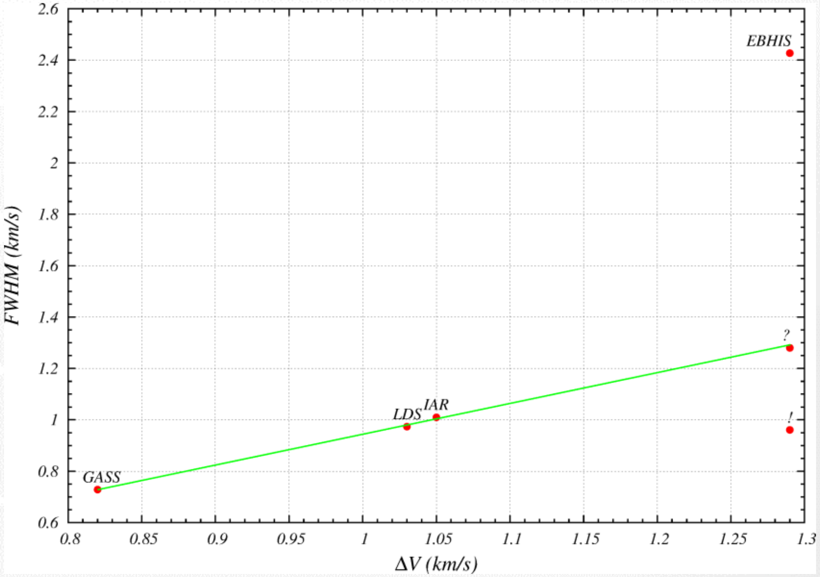

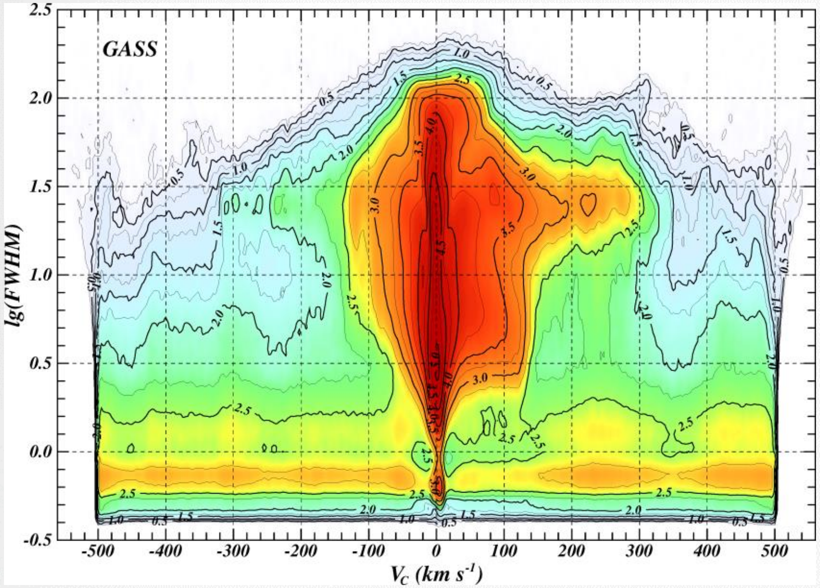

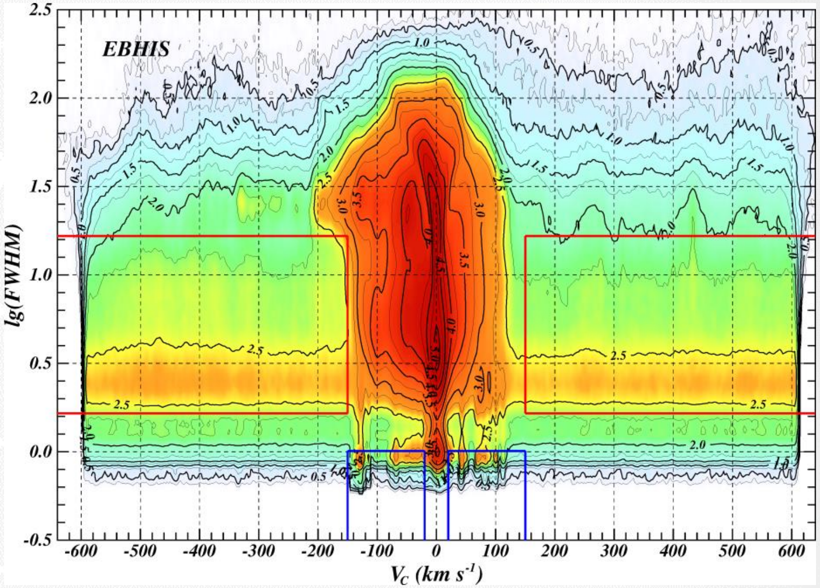

Noise – 2

- WNG correspond to the features in the observed HI profiles
  - Signal and noise regions are separated assuming that the noise has normal distribution
    - Is the noise distribution normal?
    - Is the signal and noise separation correct?
    - What may give such signal?

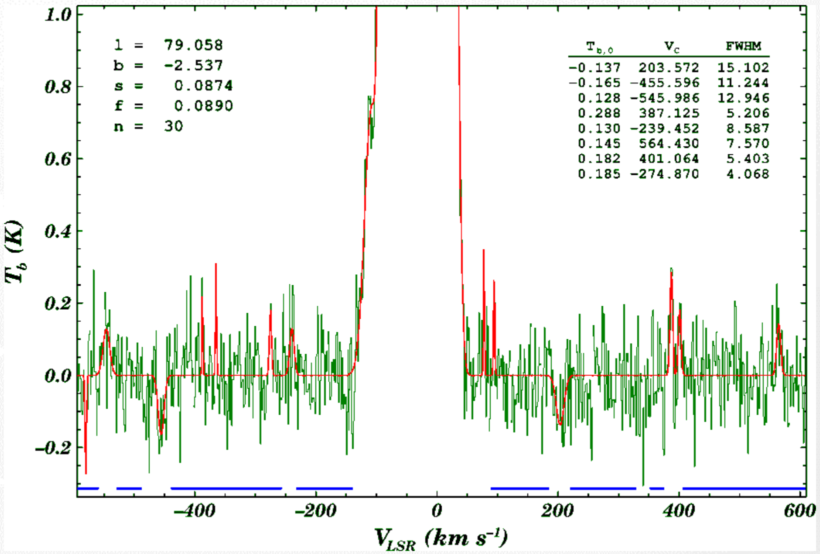

Noise – 2

- WNG correspond to the features in the observed HI profiles
  - Signal and noise regions are separated assuming that the noise has normal distribution
    - Is the noise distribution normal?
    - Is the signal and noise separation correct?
    - What may give such signal?
- NNG add unnecessary oscillations to the model profiles
  - Oscillations may appear, if we have considerably underestimated the noise level
    - Is the noise distribution normal?
    - Is the signal and noise separation correct?

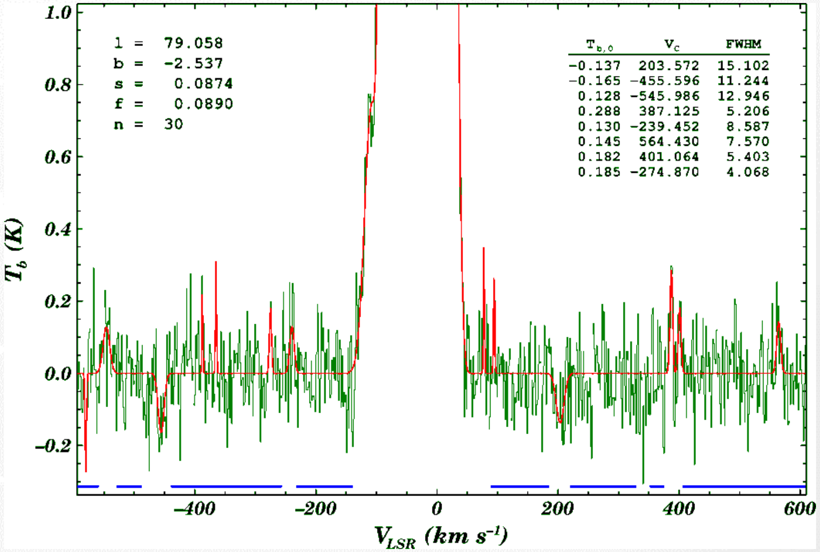

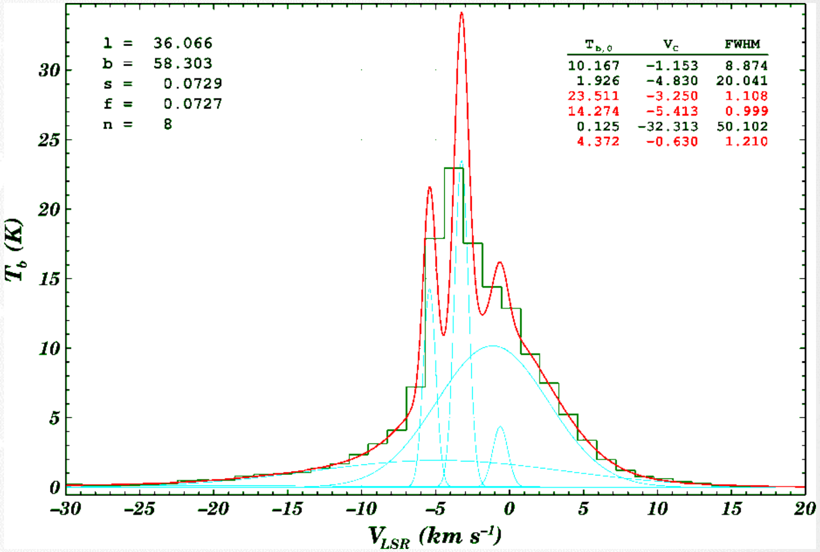

Noise – 3

- The amplitudes of the EBHIS noise follow the normal distribution even better than those of the GASS
  - At high amplitudes some unrecognized RFI may contribute to the GASS noise
  - Some noise seems to be missing in EBHIS

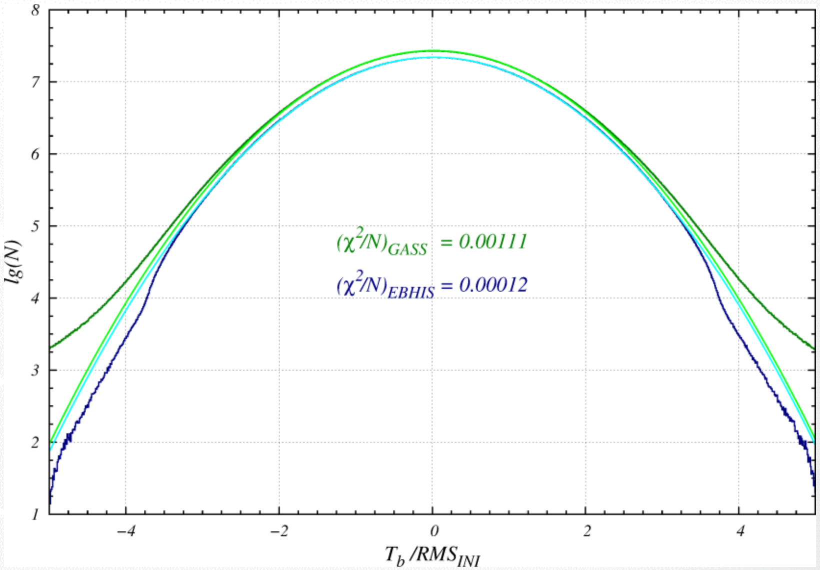

Noise – 3

- The amplitudes of the EBHIS noise follow the normal distribution even better than those of the GASS
  - At high amplitudes some unrecognized RFI may contribute to the GASS noise
  - Some noise seems to be missing in EBHIS
- $$D = \frac{\frac{N_{\text{tot,nor}}}{N_{\text{tot,obs}}} N_{i,\text{obs}} - N_{i,\text{nor}}}{N_{i,\text{nor}}}$$
  - tot – number of noise peaks above the clipping level
  - nor – normal distribution
  - obs – GASS or EBHIS observations
  - i – number of neighboring noise channels, which $|T_b|$ is above the clipping level
- In EBHIS similar noise peaks are grouped together ➔
  - Some noise is considered to be a signal. This reduces the estimates of the noise level ➔
  - Some profiles are "over fitted", resulting in oscillating models

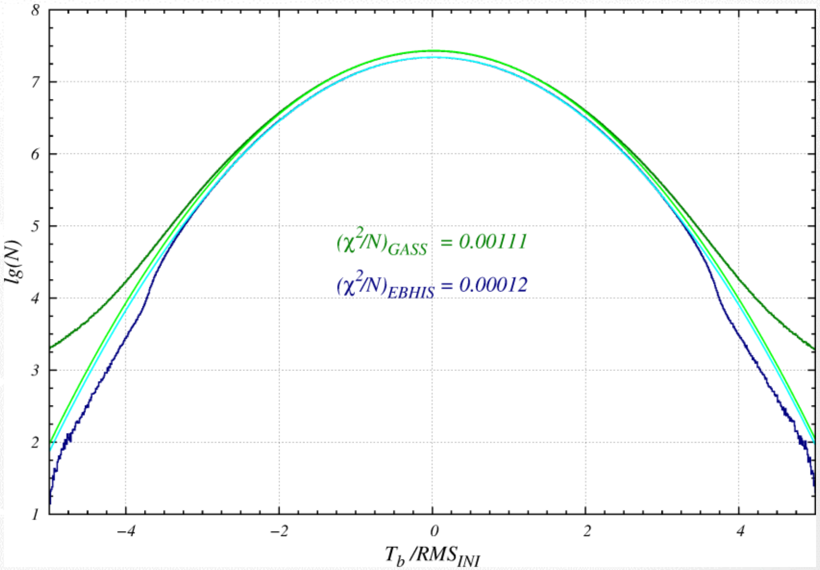

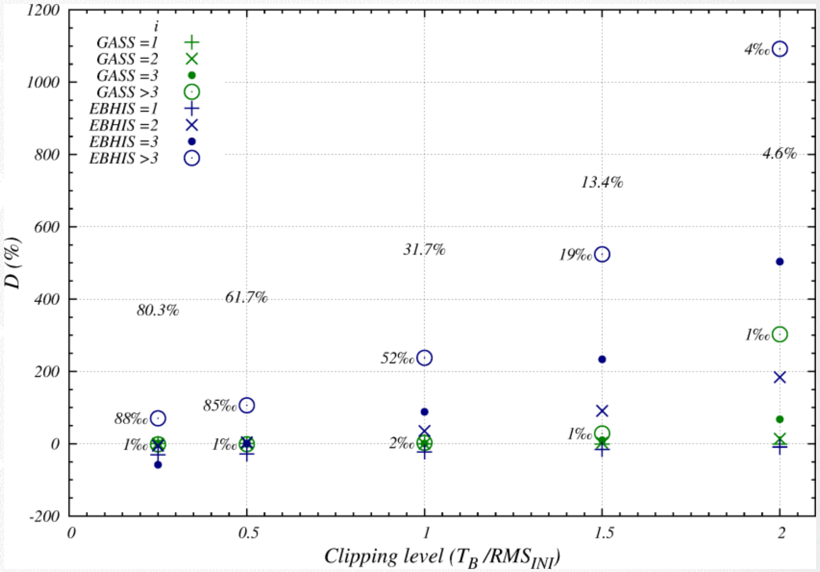

Noise – 4

- The locations of the profiles with the largest contribution from the WNG give a strange astrakhan pattern in the sky
  - To reduce the influence of differences in the observing conditions, $\mathrm{Area}/\mathrm{RMS}_{\mathrm{ini}}$ has been used for plotting

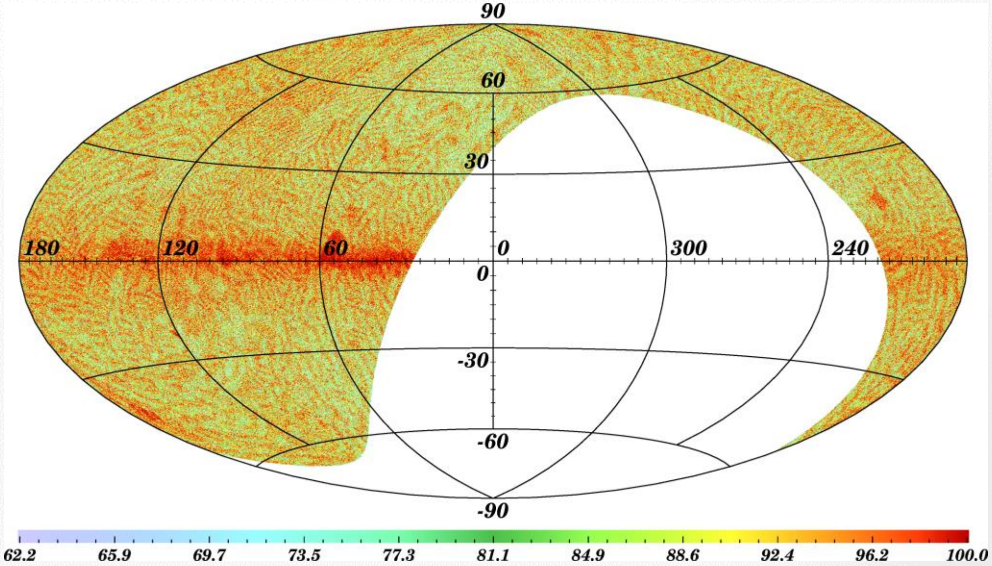

Noise – 4

- The locations of the profiles with the largest contribution from the WNG give a strange astrakhan pattern in the sky
  - To reduce the influence of differences in the observing conditions, $\mathrm{Area}/\mathrm{RMS}_{\mathrm{ini}}$ has been used for plotting
- The profiles with NNG mostly concentrate into distinct scan fields with a striped distribution inside these fields

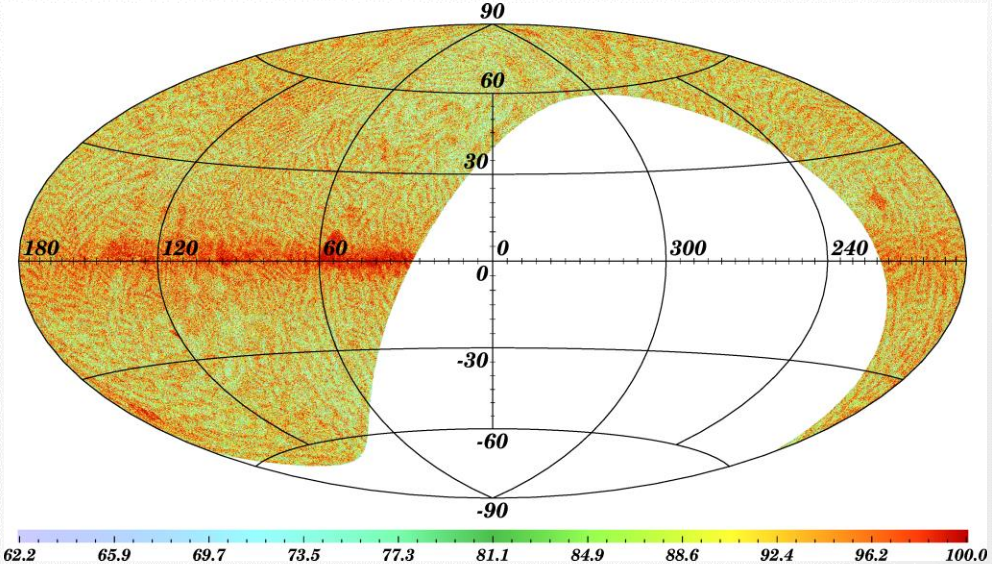

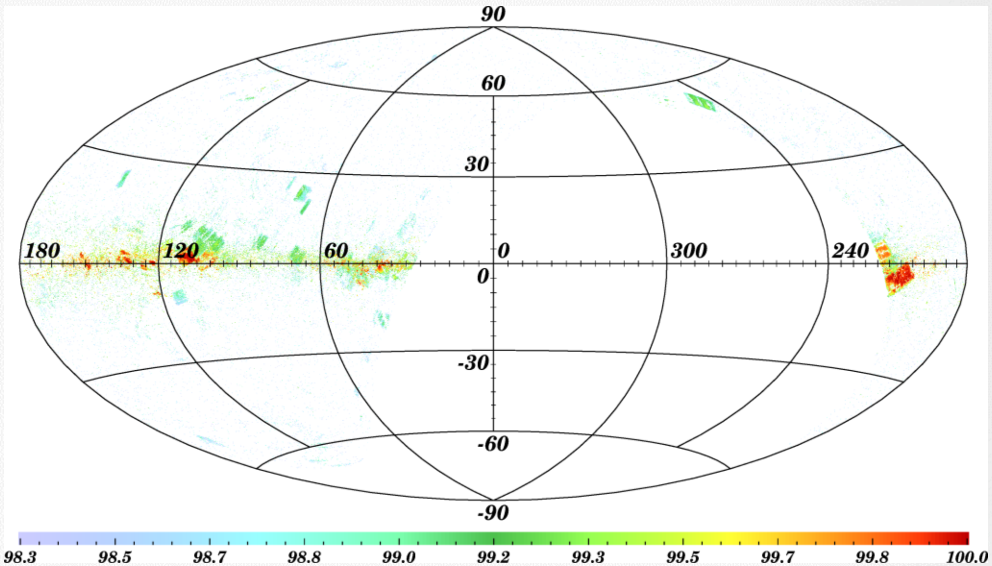

Noise – 5

- The sky distribution of $1/\sqrt{W}$
  - Different 5°×5° fields have been observed in different conditions
  - Field borders overlap
  - Observing conditions are better at higher elevations
  - Some stripes may be caused by stronger RFI

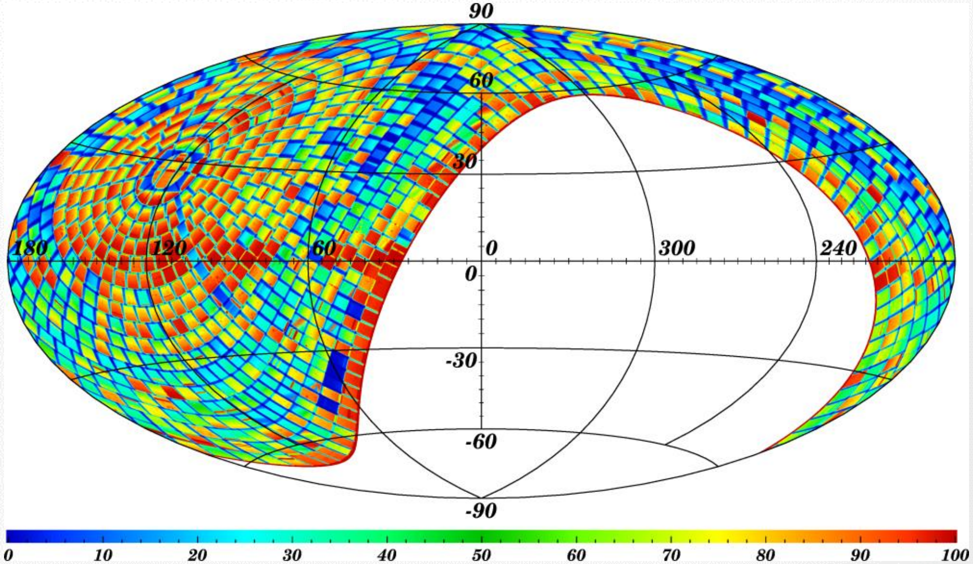

Noise – 5

- The sky distribution of $1/\sqrt{W}$
  - Different 5°×5° fields have been observed in different conditions
  - Field borders overlap
  - Observing conditions are better at higher elevations
  - Some stripes may be caused by stronger RFI
- The sky distribution of $\mathrm{RMS}_{\mathrm{ini}}$
  - 5°×5° fields are clearly visible
  - The fields contain stripes of unknown origin
  - The stripe pattern may be similar to that of WNG
- How to compensate for W?

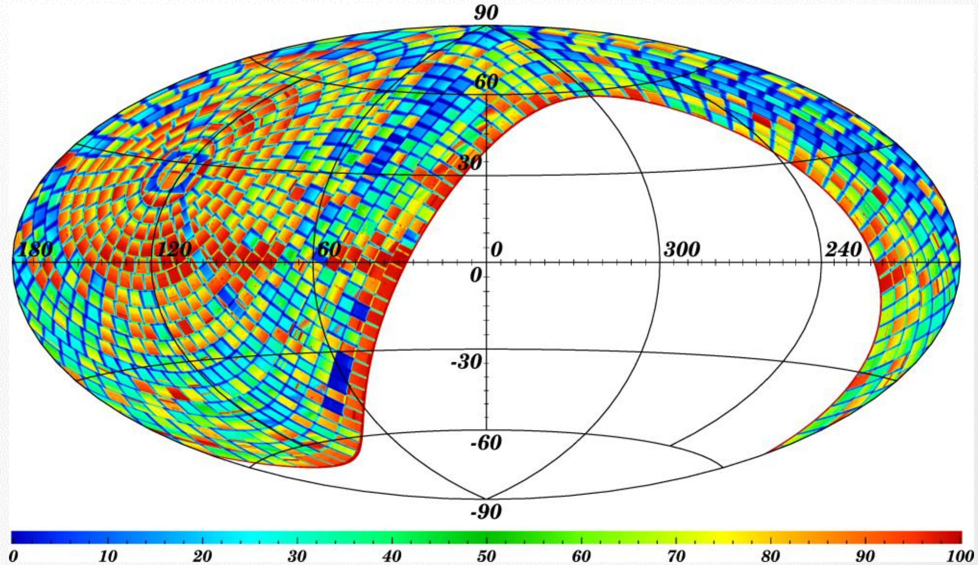

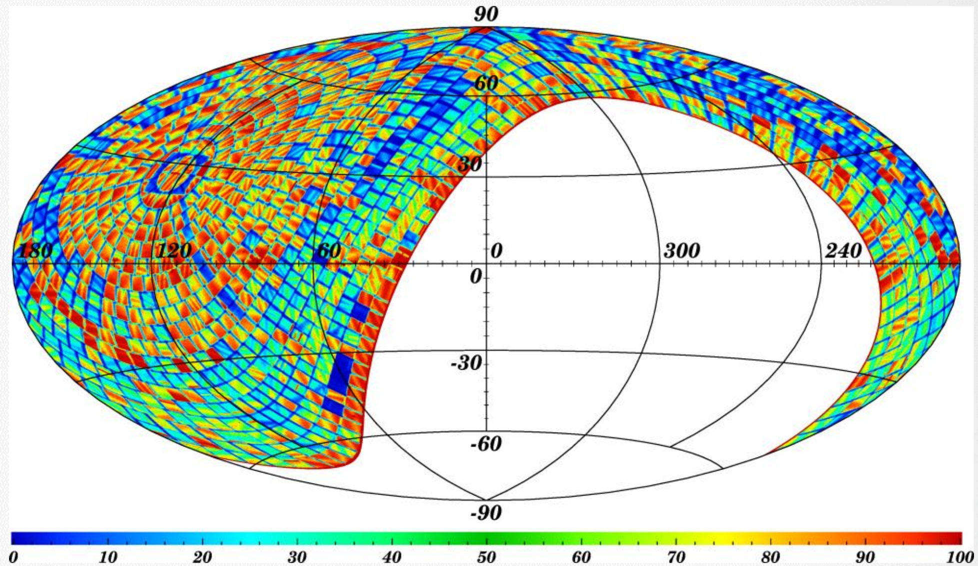

Noise – 6

- $W = 1/T_{\mathrm{rms}}^2$ ➔
- Define $R = \sqrt{W} \times \mathrm{RMS}_{\mathrm{ini}}$

Noise – 6

- $W = 1/T_{\mathrm{rms}}^2$ ➔
- Define $R = \sqrt{W} \times \mathrm{RMS_{ini}}$

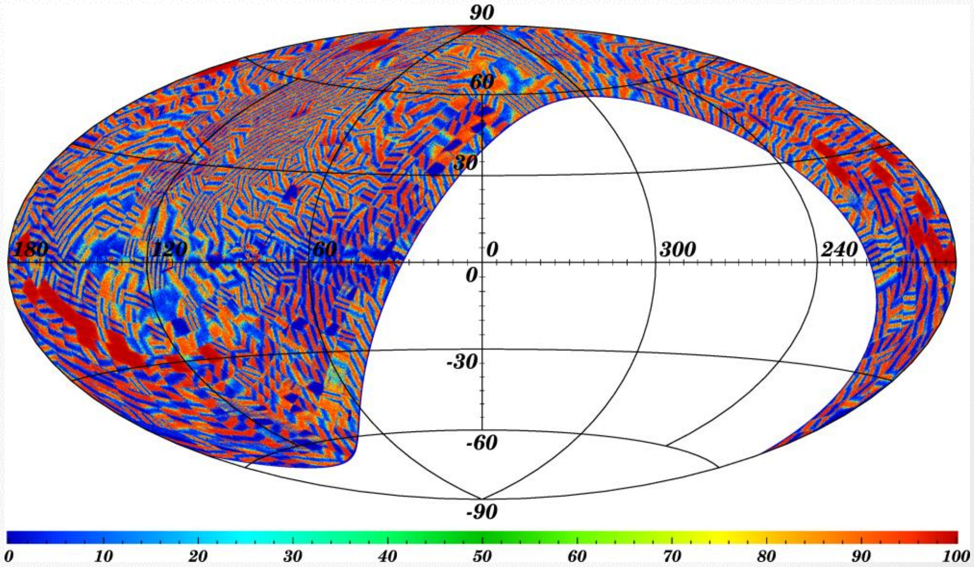

Noise – 6

- $W = 1/T_{\mathrm{rms}}^2$ ➔
- Define $R = \sqrt{W} \times \mathrm{RMS_{ini}}$
  - The pattern is similar to the one, obtained for WNG
  - It seems that the profiles with the largest WNG have the smallest values of R

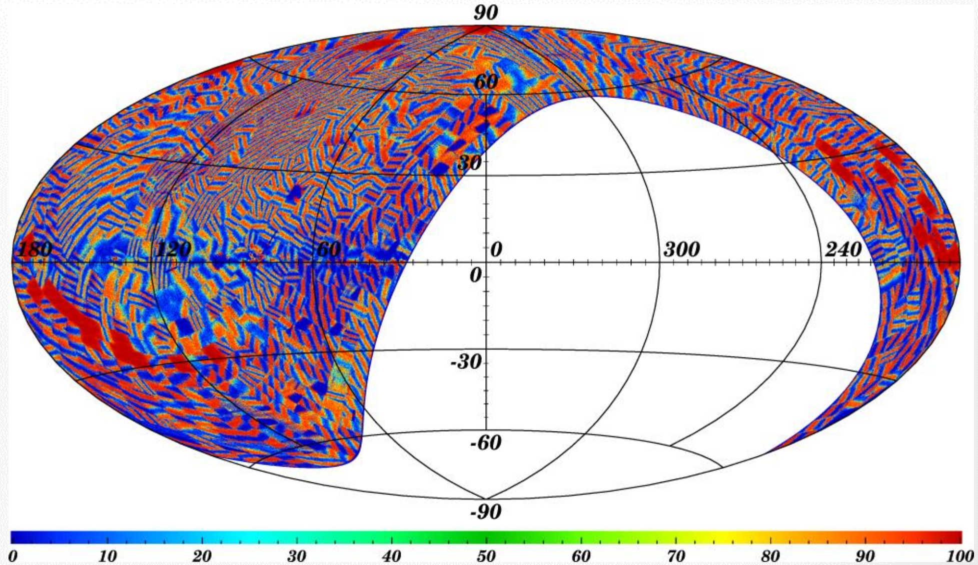

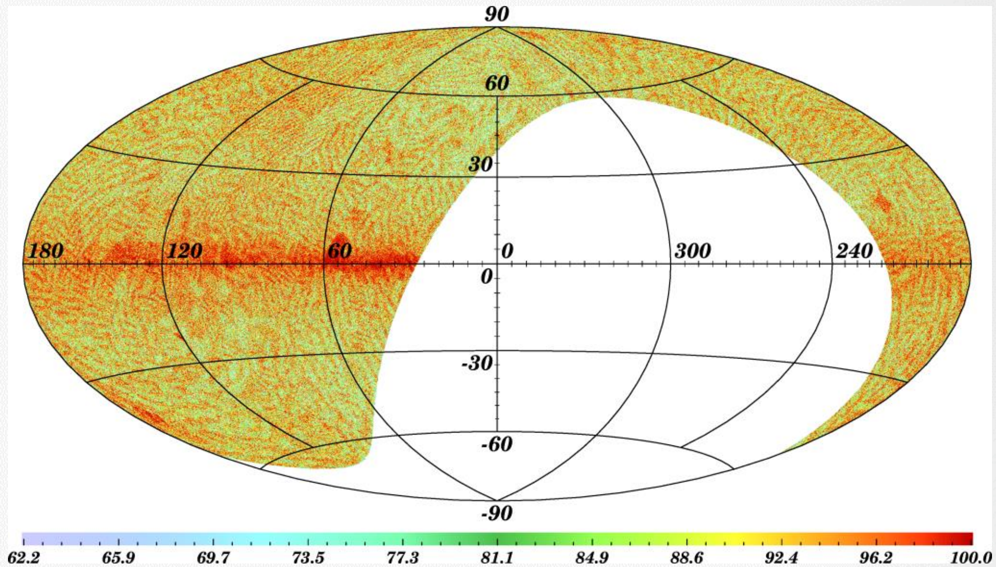

Noise – 6

- $W = 1/T_{\mathrm{rms}}^2$ ➔
- Define $R = \sqrt{W} \times \mathrm{RMS}_{\mathrm{ini}}$
  - The pattern is similar to the one, obtained for WNG
  - It seems that the profiles with the largest WNG have the smallest values of R
    - To check this, we use only the most frequent values of R
    - 1.9% ... 93.8% ... 4.3%

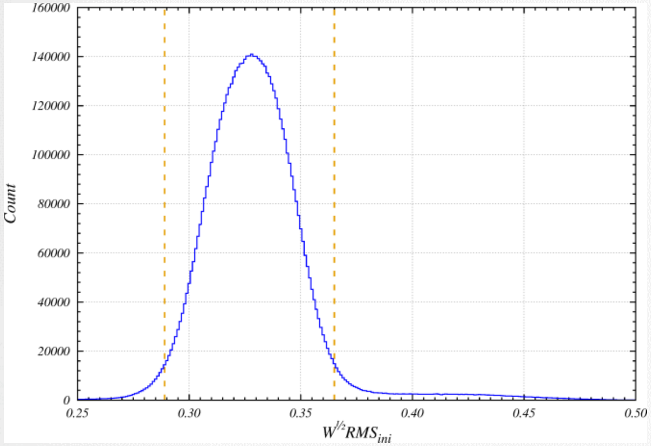

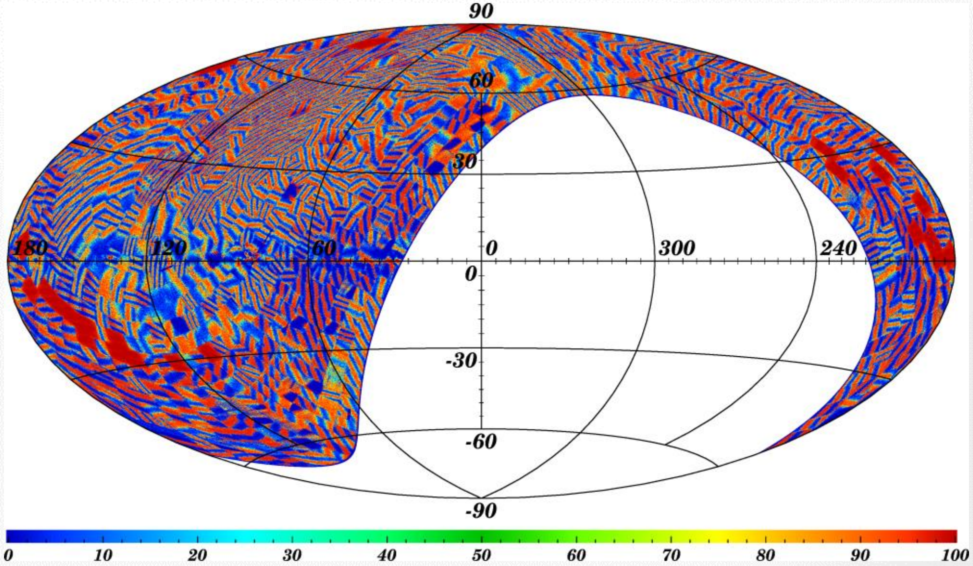

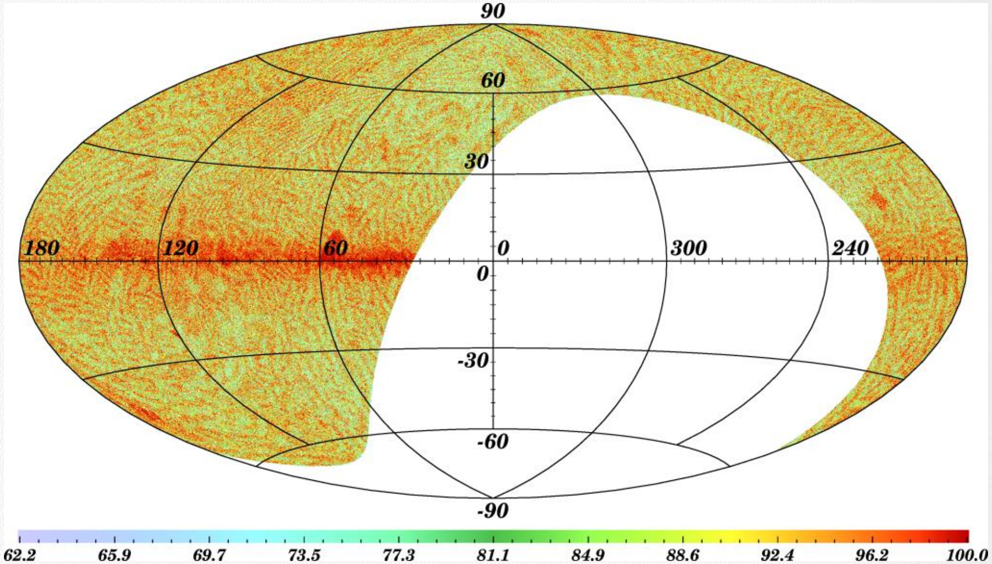

Noise – 7

- Profiles with the largest WNG correspond to the smallest values of R
- The division by $\mathrm{RMS_{ini}}$ may cause this correspondence

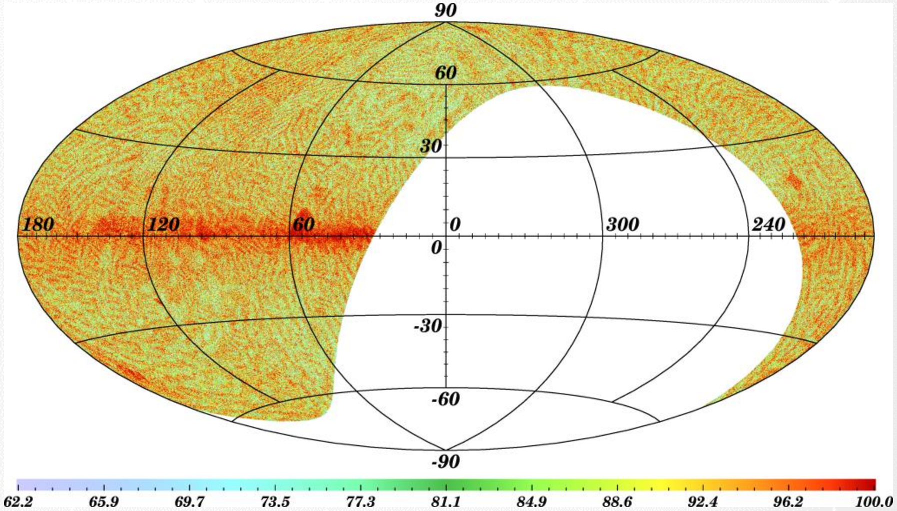

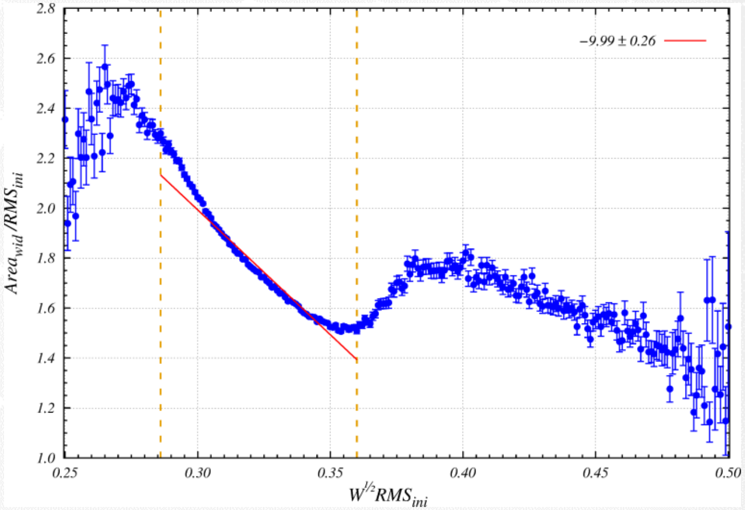

✦ www.to.ee

Noise – 7

- Profiles with the largest WNG correspond to the smallest values of R
- The division by $\mathrm{RMS_{ini}}$ may cause this correspondence
- The division explains the dependence only partially

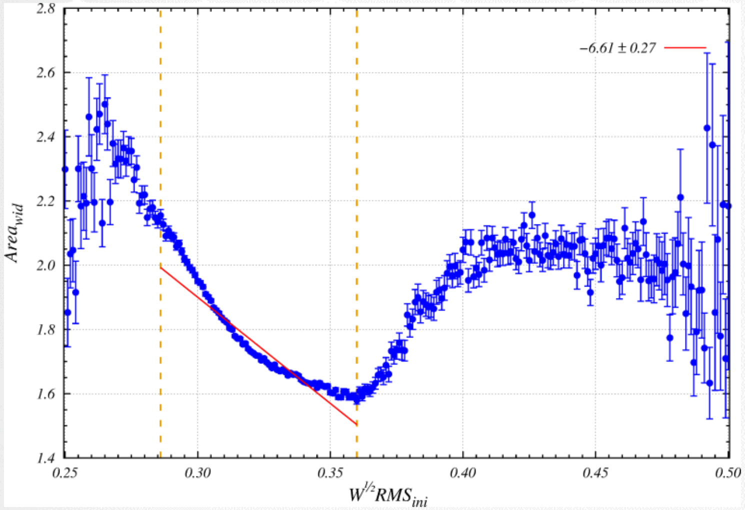

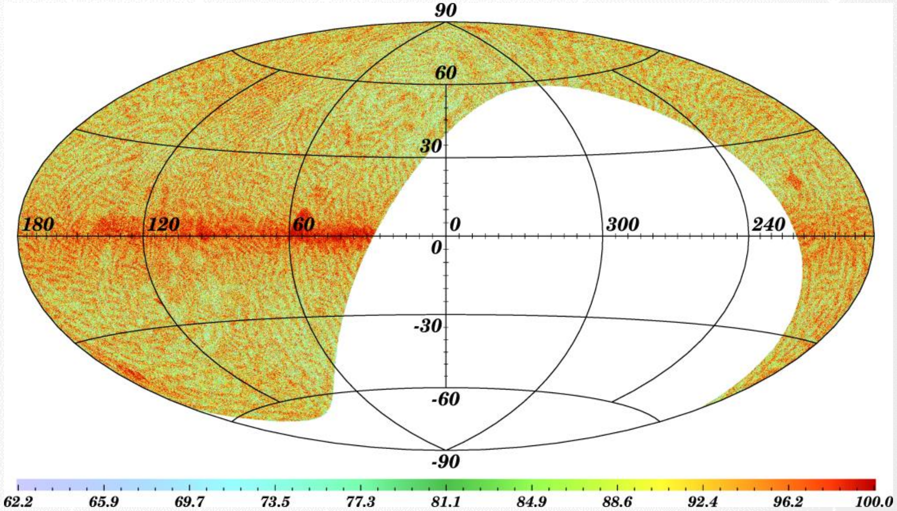

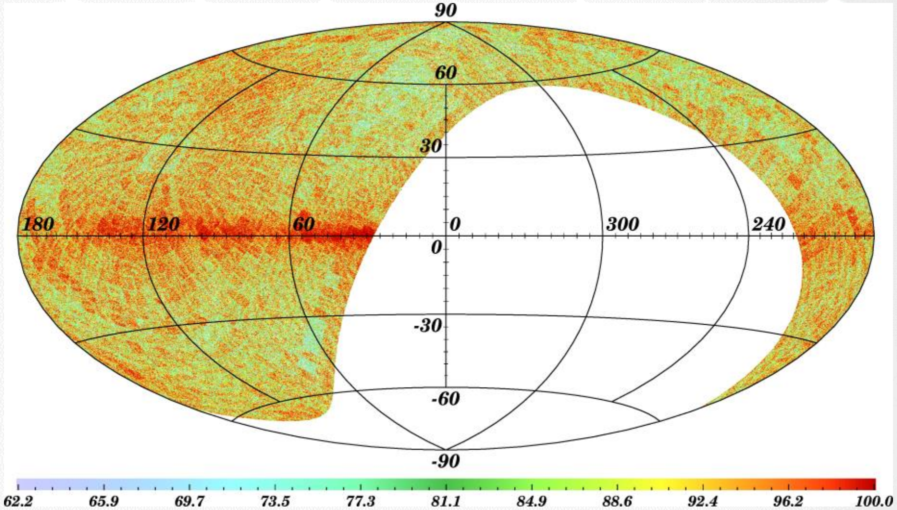

Noise – 8

- Why some profiles give NNG?
  - Grouped noise in the signal regions
  - High weights in the signal regions

Noise – 8

- Why some profiles give NNG?
  - Grouped noise in the signal regions
  - High weights in the signal regions
- Profiles with the largest NNG correspond to the smallest values of R
  - As NNG reduce the RMS of model residuals, in profiles with strong NNG the contribution of the WNG may be smaller

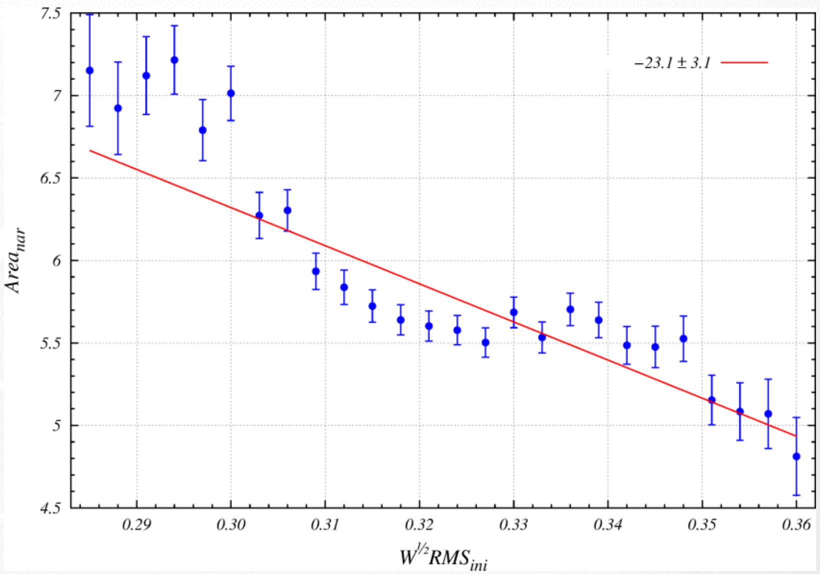

Noise – 8

- Why some profiles give NNG?
  - Grouped noise in the signal regions
  - High weights in the signal regions
- Profiles with the largest NNG correspond to the smallest values of R
  - As NNG reduce the RMS of model residuals, in profiles with strong NNG the contribution of the WNG may be smaller
- It is not clear, whether in profiles with larger NNG the contribution of the WNG is smaller

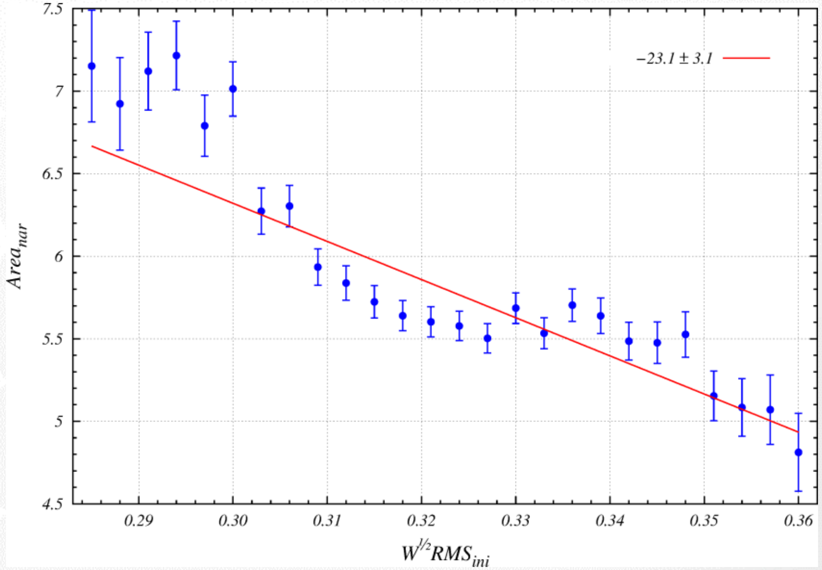

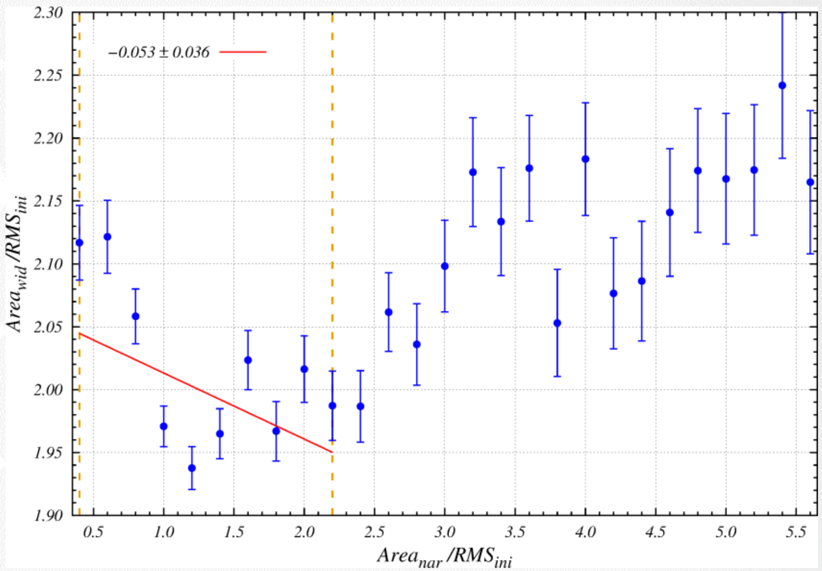

Noise – 9

- $W = 1/T_{\mathrm{rms}}^2$
- From radiometer equation $T_{\mathrm{rms}} \propto T_{\mathrm{sys}}$
- Suppose that $T_{\mathrm{rms}} \propto T_{\mathrm{b}}$
  - This ignores all corrections $(T_{\mathrm{b}} \neq T_{\mathrm{sys}})$
- Then $1/\sqrt{W} = aT_{\mathrm{b}} + b$
  - Normalization $\langle W \rangle = 1$

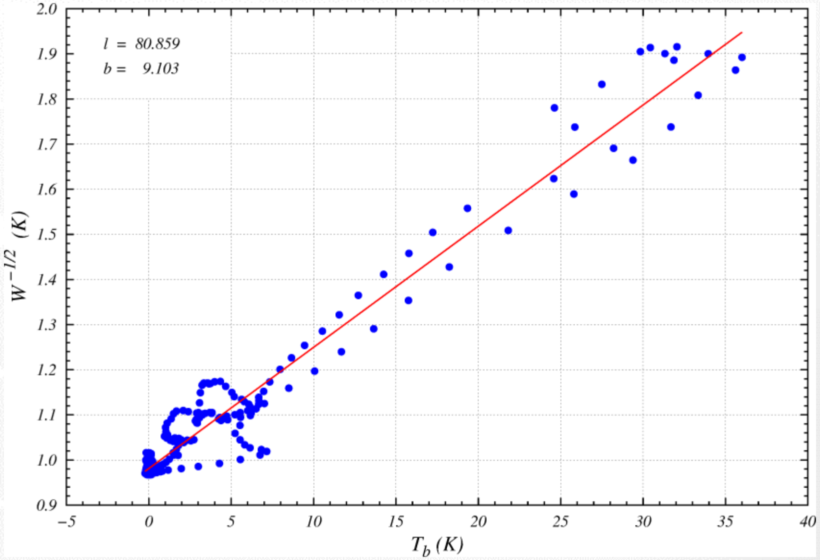

Noise – 9

- $W = 1/T_{\rm rms}^2$
- From radiometer equation $T_{\rm rms} \propto T_{\rm sys}$
- Suppose that $T_{\rm rms} \propto T_{\rm b}$
  - This ignores all corrections $(T_{\rm b} \neq T_{\rm sys})$
- Then $1/\sqrt{W} = aT_{\rm b} + b$
  - Normalization $\langle W \rangle = 1$
- On average, the values of parameter a are smaller for profiles with larger NNG ➔
  - NNG appear in the profiles for which the weights of the signal regions are relatively high (the weights decrease with increasing signal strength more slowly than in other profiles with underestimated $\mathrm{RMS_{ini}}$)

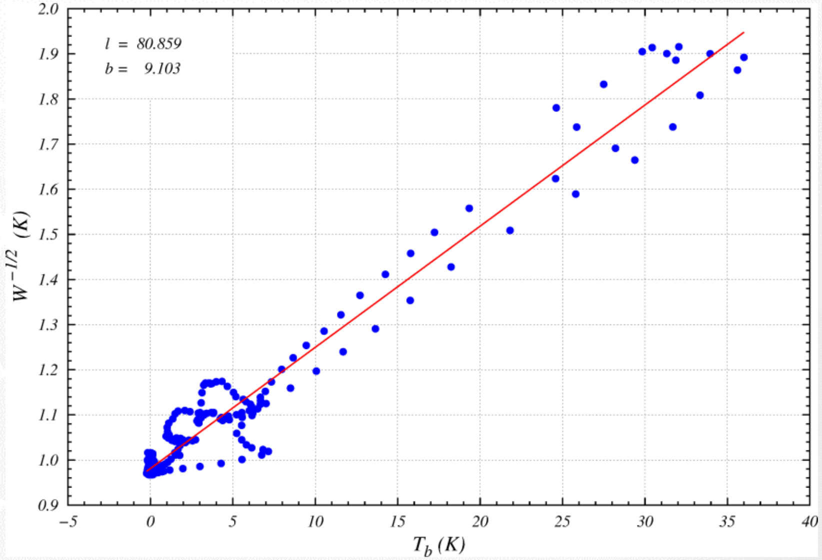

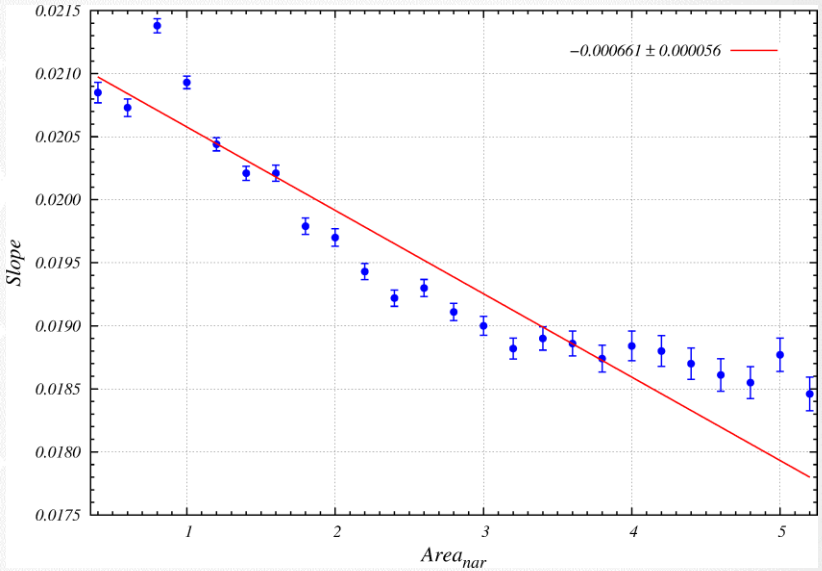

Conclusions

- Velocity corrections for the weights have now been applied
- Average baseline level has been improved
- The cause of the noise correlations is still unknown
  - “My guess is that the answer lies somewhere in the hardware used for the survey”
- Present noise characteristics reduce the value of the survey for studying:
  - High- and intermediate velocity HI clouds (2006 A&A 455 481, 2008 A&A 483 461)
  - Very cold HI clouds (2010 A&A 514 A27, 2013 A&A 552 A108, 2016 ApJ)
  - Everything else, for which the independently random distribution of the noise is required
- The Gaussian decomposition gives expected results from unexpected data
- First data release: 2016 A&A 585 A41